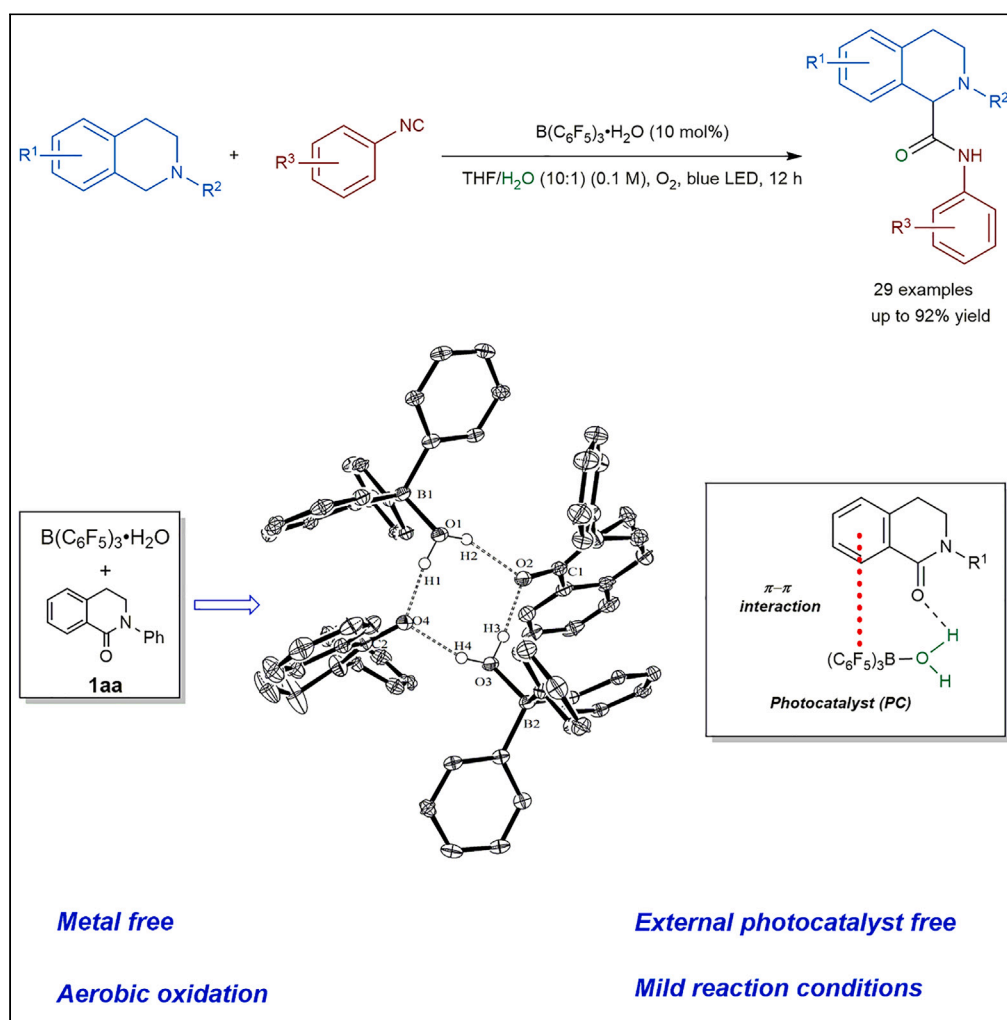


Article

Synergistic effect of hydrogen bonds and π - π interactions of $B(C_6F_5)_3 \cdot H_2O$ /amides complex: Application in photoredox catalysisShi-Jun Wang,
Long Wang,
Xiang-Ying Tang

xytang@hust.edu.cn

HighlightsAerobic oxidation under
visible light conditionsNo need for an external
photocatalystHydrogen bonds and π - π
interactions between
 $B(C_6F_5)_3 \cdot H_2O$ and amides
were identified

Article

Synergistic effect of hydrogen bonds and π - π interactions of $B(C_6F_5)_3 \cdot H_2O$ /amides complex: Application in photoredox catalysisShi-Jun Wang,¹ Long Wang,¹ and Xiang-Ying Tang^{1,2,*}

SUMMARY

$B(C_6F_5)_3 \cdot H_2O$ has been long recognized as a common Brønsted acid. The lack of X-ray crystal structure of $B(C_6F_5)_3 \cdot H_2O$ with other substrates has greatly limited the development of a new catalytic mode. In this work, a complex of $B(C_6F_5)_3 \cdot H_2O$ and amide 2-phenyl-3,4-dihydroisoquinolin-1(2H)-one with hydrogen bonds and π - π interactions is characterized by X-ray diffraction. Such noncovalent interactions in solution also exist, as verified by NMR, UV-Vis absorption, and fluorescence emission measurements. Moreover, the mixture of amide 2-phenyl-3,4-dihydroisoquinolin-1(2H)-one and $B(C_6F_5)_3 \cdot H_2O$, instead of other tested Brønsted acids, shows a tailing absorption band in the visible light region (400–450 nm). Based on the photoactive properties of the complex, a photoredox catalysis is developed to construct α -aminoamides under mild conditions.

INTRODUCTION

Tris(pentafluorophenyl)borane, $B(C_6F_5)_3$, as a main group Lewis acid, has been deeply investigated during the last decade.^{1–8} Besides, with the discovery of crystal structure of $B(C_6F_5)_3$ with various molecules,^{9–18} the catalytic mode of $B(C_6F_5)_3$ was further revealed.^{19–31} On the other hand, owing to the moisture sensitivity of $B(C_6F_5)_3$, it is likely that the Brønsted acid $B(C_6F_5)_3 \cdot H_2O$ acts as the real catalyst.^{32,33} Although, there are some reports indicating that this effect can be attenuated in frustrated Lewis pairs (FLP) chemistry,^{34–37} the strict anhydrous conditions are still necessary in most $B(C_6F_5)_3$ catalyzed transformations.

$B(C_6F_5)_3 \cdot H_2O$ is a strong Brønsted acid^{38–40} and the strength is similar to that of HCl in acetonitrile.³⁸ It has been reported that $B(C_6F_5)_3 \cdot H_2O$ shows superior activity than other Brønsted acids in some transformations.^{41–45} However, it is difficult to identify the real catalytic species under moist conditions, because Lewis acid and water-mediated pathways are competitive.^{34–37,41–47} In the water-tolerant FLP-catalyzed hydrogenation, for instance, ethers could competitively replace water to coordinate with $B(C_6F_5)_3$ (Figure 1A).^{34–37} Meanwhile, $B(C_6F_5)_3 \cdot H_2O$ are mainly considered as a hydrogen bond donor. For instance, in the $B(C_6F_5)_3 \cdot H_2O$ catalyzed ring opening reactions of epoxides,^{46,47} hydrogen bond interactions between $B(C_6F_5)_3 \cdot H_2O$ and epoxides/alcohols are revealed by microkinetic modeling and density functional theory calculations (Figure 1B).⁴⁴ Even though existing studies could account for the hydrogen bond interactions, other noncovalent interactions are barely considered. Thus, the direct and intuitive evidences such as X-ray single crystal diffraction are highly desirable.

A myriad of X-ray structures of four-coordinated complex via anhydrous $B(C_6F_5)_3$ were reported.^{9–18} In contrast, there have been very limited reports involving X-ray structures of $B(C_6F_5)_3 \cdot H_2O$ with other molecules,^{38–40} resulting in difficulties understanding the difference between $B(C_6F_5)_3 \cdot H_2O$ and other Brønsted acids. Herein, we wish to report an interesting X-ray crystal structure (C1) of $B(C_6F_5)_3 \cdot H_2O$ and 2-phenyl-3,4-dihydroisoquinolin-1(2H)-one (**1aa**), forming through intermolecular hydrogen bonds and π - π interactions. Meanwhile, the mixture of $B(C_6F_5)_3 \cdot H_2O$ and **1aa** in tetrahydrofuran (THF) solution showed reinforcement both in UV-Vis absorption and fluorescence emission. On the basis of these observations, a photoredox oxidation reaction was developed using the combination of $B(C_6F_5)_3 \cdot H_2O$ and **1aa** as the photocatalyst.

¹School of Chemistry and Chemical Engineering, Hubei Key Laboratory of Bioinorganic Chemistry and Materia Medica and Semiconductor Chemistry Center, Huazhong University of Science and Technology, Wuhan, Hubei, China

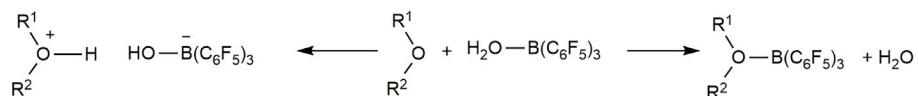
²Lead contact

*Correspondence: xytang@hust.edu.cn

<https://doi.org/10.1016/j.isci.2023.106528>



A water-tolerant FLP-catalysis



B water- and alcohol-mediated catalysis

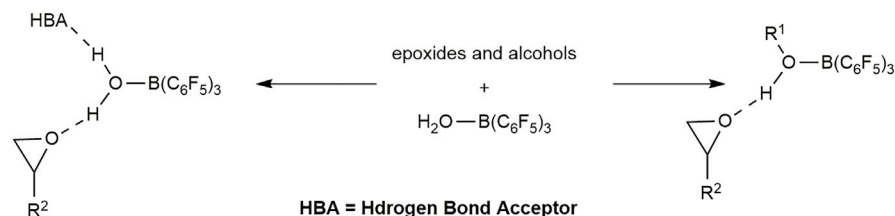


Figure 1. Competitive boron Lewis acid, water- and alcohol-mediated pathways

RESULTS AND DISCUSSION

Identify noncovalent interactions between $B(C_6F_5)_3 \cdot H_2O$ and amide **1aa**

The crystals of **C1** suitable for X-ray crystal structure analysis were obtained by slowly solvent evaporation of the solution of **1aa** and $B(C_6F_5)_3 \cdot H_2O$ (1:1) in dichloromethane (Figure 2). The B–O bond lengths in **C1** are 1.5692(19) and 1.5557(19) Å, slightly shorter than that in aqua complexes of $B(C_6F_5)_3$.^{38–40} Correspondingly, the C=O bond lengths are elongated to be 1.2579(19) and 1.2622(19), respectively.^{48,49}

As can be seen from Figure 3, there are two π - π interactions between $-C_6F_5$ of $B(C_6F_5)_3$ and phenyl moiety of **1aa**. The twist angles of aromatic rings are 21.21(14) and 1.32(16) degree respectively. Besides, the distances between centroids are in the range of 3.30–3.80 Å.⁵⁰

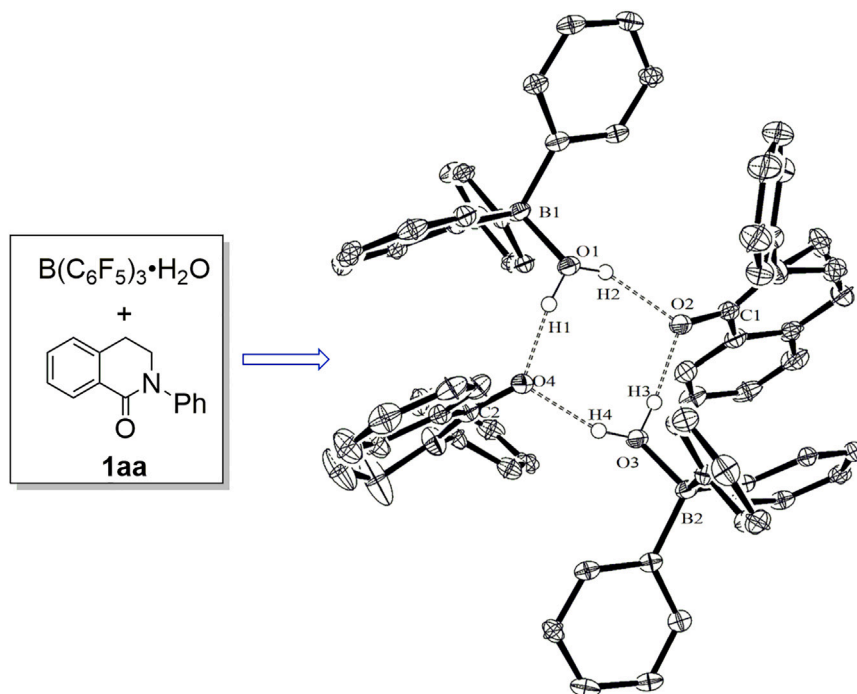


Figure 2. X-ray crystal structure of **C1 ($B(C_6F_5)_3 \cdot H_2O + 1aa$)**

F atoms and part of the hydrogen atoms are omitted for clarity. Selected bond distances (Å): B1–O1 1.5692(19), B2–O3 1.5557(19), C1–O2 1.2579(19), C2–O4 1.2622(19). CCDC (2207426).

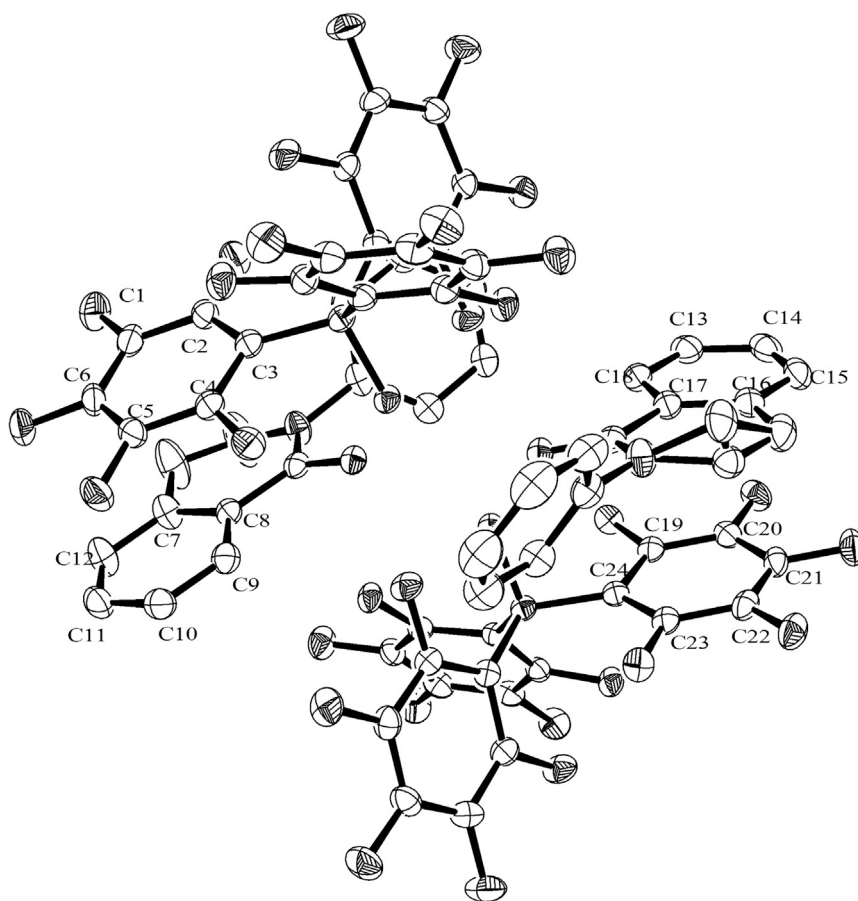


Figure 3. π - π interactions

Hydrogen atoms are omitted for clarity. Selected distances (Å) and angles (deg): plane centroid of C1–C6 to plane centroid of C7–C12 3.8065(10), plane centroid of C1–C6 to plane C7–C12 3.4126(16), plane to plane twist angle 21.21(14); plane centroid of C13–C18 to plane centroid of C19–C24 3.5511(10), plane centroid of C13–C18 to plane C19–C24 3.3748(12), plane to plane twist angle 1.32(16).

There are four oxygen atoms and four hydrogen atoms, forming an eight-membered ring in the conformation of boat-chair via hydrogen bond possessing the lowest transannular strain and energy (Figure 4).^{51,52} The O ... O distances in O–H ... O hydrogen bond system range is 2.5627(15)–2.7583(15) Å, relatively shorter than the reported intermolecular O ... O distances (2.70–3.00 Å),^{53,54} suggesting the existence of stronger hydrogen bonds in crystal C1.

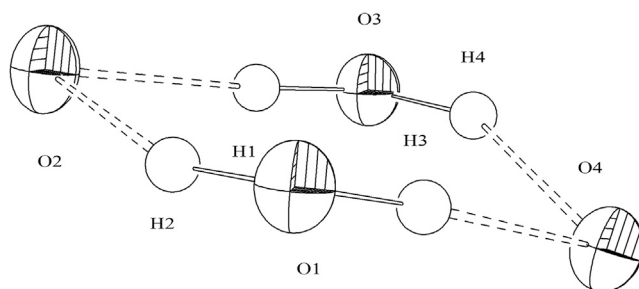


Figure 4. Structure analysis of eight-membered rings of hydrogen bond

Selected bond distances (Å): O1–H1 0.89(3), O1–H2 0.86(3), O3–H3 0.86(3), O3–H4 0.90 (3), O4 ... H1 1.69(3), O2 ... H2 1.97(3), O2 ... H3 1.71(3), O4 ... H4 1.83(3), O1 ... O2 2.7583(15), O2 ... O3 2.5627(15), O3 ... O4 2.6578(15), O1 ... O4 2.5659(15).

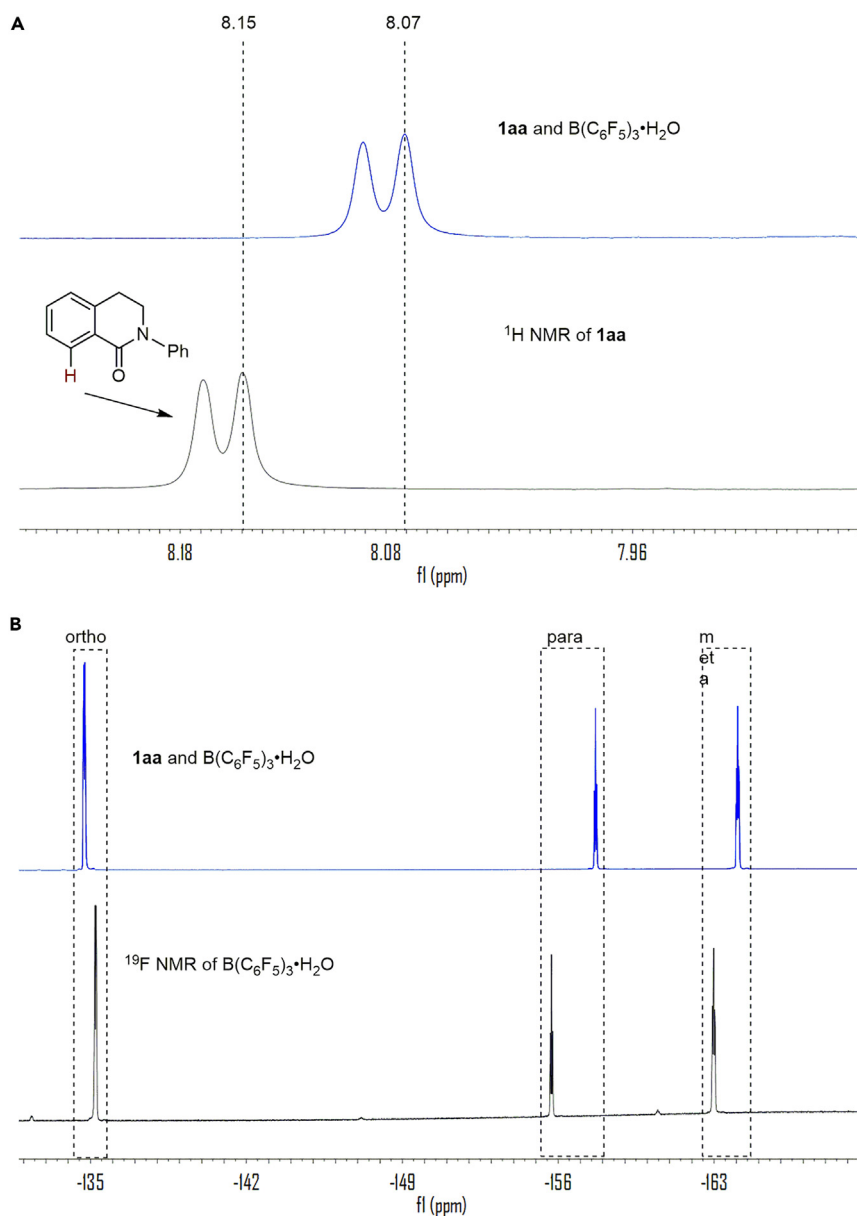


Figure 5. NMR experiments

0.05 mmol **1aa** was dissolved in 0.6 mL deuterated chloroform (CDCl₃).

(A) **1aa** (black); **1aa**/B(C₆F₅)₃·H₂O (1:1) (blue).

(B) B(C₆F₅)₃·H₂O (black); **1aa**/B(C₆F₅)₃·H₂O (1:1) (blue).

Encouraged by the above discoveries in **C1**, we considered that similar interactions might exist in solution. Compound **1aa** showed a ¹H NMR resonance at 8.15 ppm in CDCl₃ (Figure 5A, black curve). With the addition of B(C₆F₅)₃·H₂O (1.0 equiv), the resonance shifted to 8.07 ppm (Figure 5A, blue curve), indicating the formation of π-π interactions in solution.^{55,56} The ¹⁹F NMR of B(C₆F₅)₃·H₂O also changed on the addition of **1aa**. The original peaks of B(C₆F₅)₃·H₂O were observed at -135.2, -155.7 and -163.0 ppm (Figure 5B, black curve).⁴¹ Upon addition of **1aa** (1.0 equiv), the characteristic peaks changed to -134.7, -157.7 and -164.0 ppm, respectively (Figure 5B, blue curve). According to previous reports,^{36–38,41,42} intermolecular hydrogen bonds should exist between **1aa** and B(C₆F₅)₃·H₂O in solution.

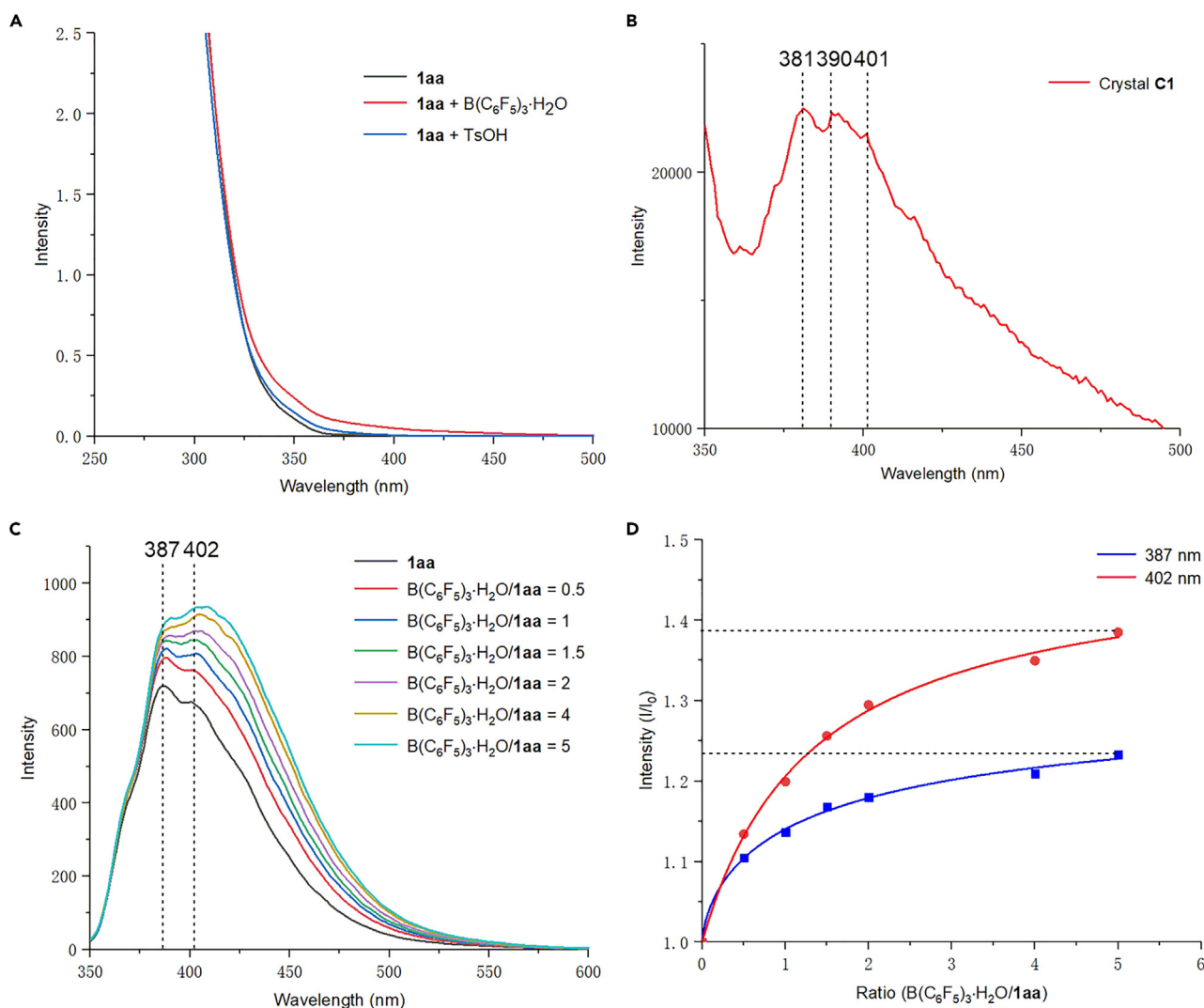


Figure 6. UV-Vis absorption and fluorescence emission measurements

(A) **1aa** in THF (10^{-3} M, black); **1aa** and $B(C_6F_5)_3 \cdot H_2O$ (1:1) in THF (10^{-3} M, red); **1aa** and *p*-toluenesulfonic acid (TsOH) (1:1) in THF (10^{-3} M, blue).
(B) Fluorescence emission spectra of **C1**, excitation wavelength, 330 nm.
(C) Fluorescence emission spectra of **1aa** in THF (10^{-4} M), $B(C_6F_5)_3 \cdot H_2O$ were added to the solution of **1aa**, excitation wavelength, 330 nm.
(D) Emission intensity, 387 nm and 402 nm.

In tetrahydrofuran solution, **1aa** as well as the mixture of **1aa** and *p*-toluenesulfonic acid (TsOH), show no absorption in visible light region, respectively (Figure 6A, black and blue curves). Similarly, using other Brønsted acids instead of TsOH as hydrogen bond donors, such as phenylboronic acid, cyclohexanecarboxylic acid, and methanesulfonic acid, the corresponding mixtures also show no absorption in the visible light region (see supplemental information for detail, Figure S4). However, the mixture of **1aa** and $B(C_6F_5)_3 \cdot H_2O$ exhibits a tailing band from 400 to 450 nm (Figure 6A, red curve).

The fluorescence emission measurements of **C1** and **1aa**/ $B(C_6F_5)_3 \cdot H_2O$ were attempted. The solid fluorescence emission spectrum of **C1** showed three peaks at 381 nm, 390 nm, and 401 nm (Figure 6B). Similar emission peaks were observed in solution. There were two fluorescent peaks at 387 nm and 402 nm, which are enhanced in terms of the emission intensity by increasing the $B(C_6F_5)_3 \cdot H_2O$ fraction (Figure 6C). When the ratio of $B(C_6F_5)_3 \cdot H_2O/1aa$ is 1.5:1, the emission intensity was comparable at 387 nm and 402 nm. With the addition of $B(C_6F_5)_3 \cdot H_2O$, the emission intensity at 402 nm gradually became stronger than the emission intensity at 387 nm, indicating that the rotation of aromatic rings was more restricted because of

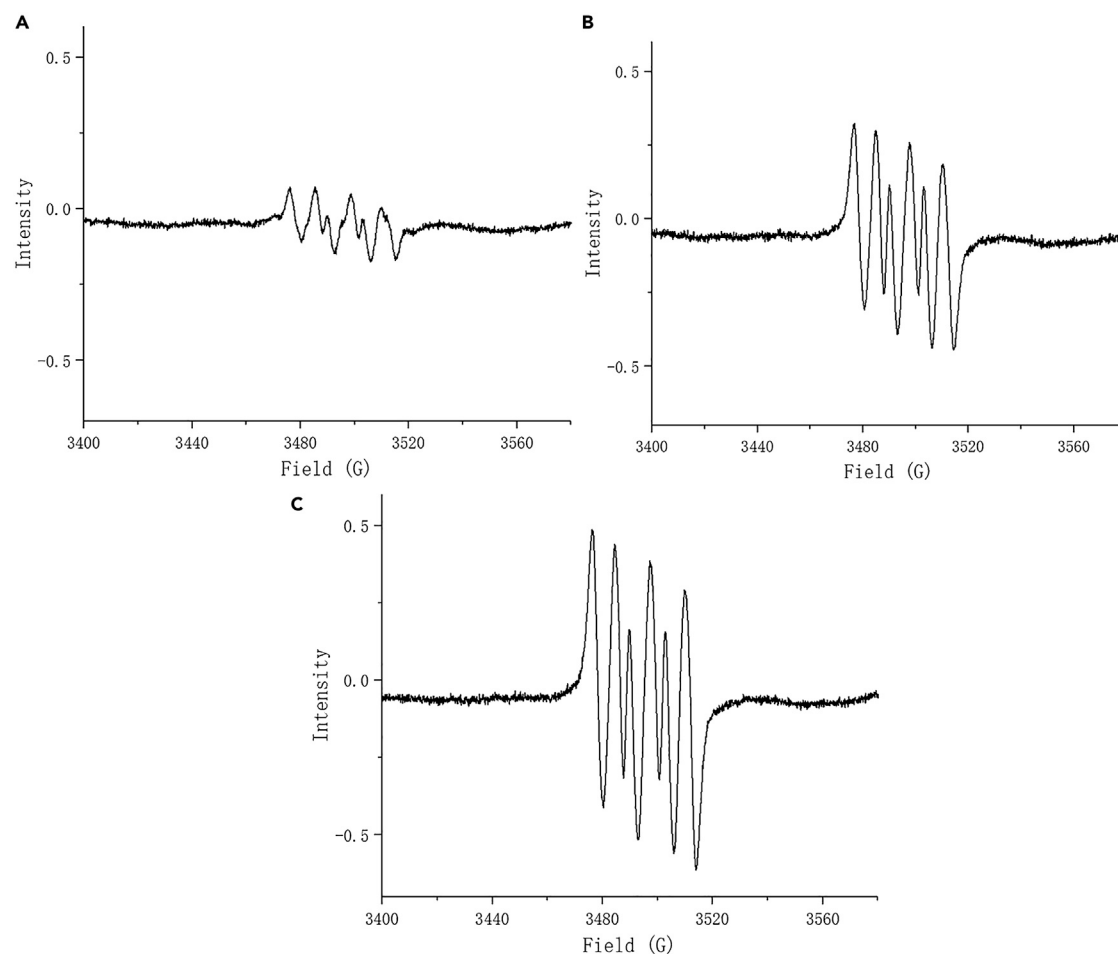


Figure 7. EPR measurements

0.05 mmol scale, **1aa**/DMPO/ $B(C_6F_5)_3 \cdot H_2O$ (1:1:1) in THF (1 mL) under air.

(A) in the dark.

(B) irradiated by blue LEDs for 2 min.

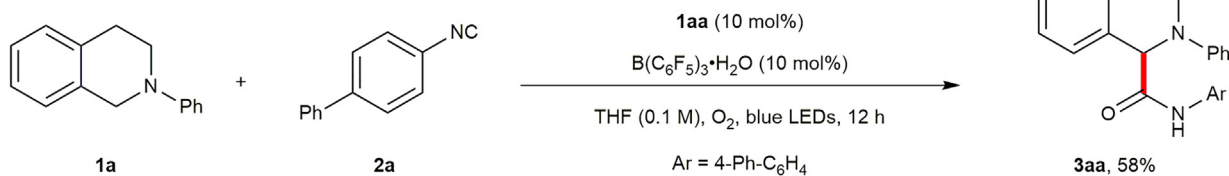
(C) irradiated by blue LEDs for 5 min.

increased π - π interactions.^{55,56} In comparison to $B(C_6F_5)_3 \cdot H_2O$ /**1aa** (5:1) and **1aa**, the fluorescence emission intensities at 387 nm and 402 nm were enhanced by 23% and 38%, respectively (Figure 6D).

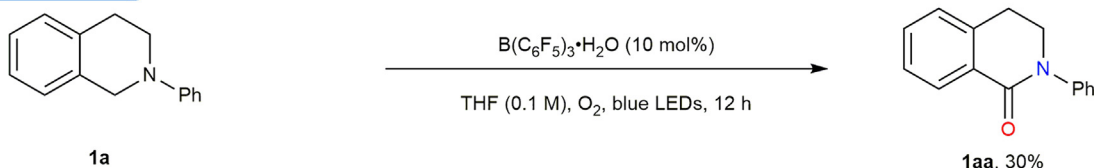
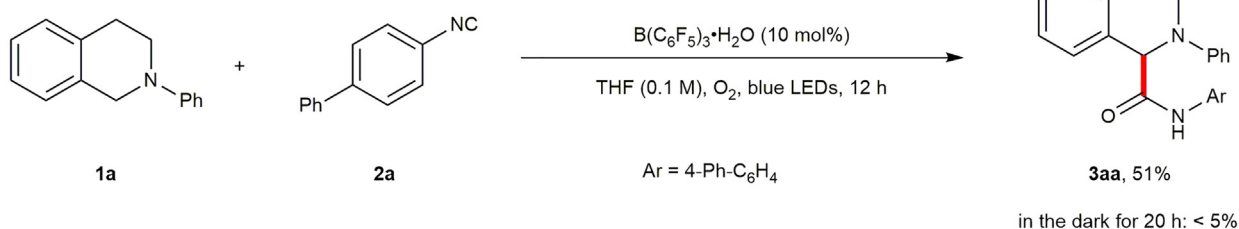
To further explore the properties of mixture of $B(C_6F_5)_3 \cdot H_2O$ and **1aa**, electron paramagnetic resonance (EPR) measurements were conducted. As can be seen in Figure 7, directly subjecting the THF solution of **1aa**, $B(C_6F_5)_3 \cdot H_2O$ and 5,5-dimethyl-1-pyrroline-*N*-oxide (DMPO) to EPR, a weak radical signal was detected (Figure 7A). A strong signal appeared when the above solution was irradiated by blue light for 2 min (Figure 7B). As the irradiation time was extended to 5 min, further enhancement was observed (Figure 7C). According to previous reports, DMPO- O_2^- species is formed ($\alpha_N = 13.1$ G, $\alpha_H = 9.1$ G), indicating that the mixture of $B(C_6F_5)_3 \cdot H_2O$ and **1aa** can activate molecular oxygen probably through energy transfer on visible light irradiation.^{57–60}

These observations of the complex of $B(C_6F_5)_3 \cdot H_2O$ and **1aa** inspired us to further exploit its catalytic potential in photoredox catalysis. Therefore, the reaction of *N*-phenyl-tetrahydroisoquinoline (**1a**) and 4-isocyano-1,1'-biphenyl (**2a**) was investigated. As expected, the reaction gave corresponding product **3aa** in 58% yield in THF using 10 mol % of $B(C_6F_5)_3 \cdot H_2O$ /**1aa** as photocatalyst (Figure 8A). Besides, in the absence of isocyanide, **1a** could be converted to **1aa** in 30% yield catalyzed by $B(C_6F_5)_3 \cdot H_2O$, with 61% **1a** recovered (Figure 8B). Thus, when **1a** and **2a** were treated by $B(C_6F_5)_3 \cdot H_2O$, the desired product

A photoredox catalysis



B transformation of 1a to 1aa

C photoredox catalysis by B(C₆F₅)₃·H₂O and in situ formed 1aaFigure 8. Catalytic properties of B(C₆F₅)₃·H₂O and 1aa

(A) C1 Catalysis Experiment: 1a (0.15 mmol), 2a (0.1 mmol).

(B) generate 1aa via 1a direct oxidation, 1a (0.1 mmol).

(C) 1a was found to generate to 1aa, subsequently combined with B(C₆F₅)₃·H₂O to catalyze the reaction. 1a (0.15 mmol), 2a (0.1 mmol).

3aa could still be obtained in 51% yield (Figure 8C). Meanwhile, only trace amount of 3aa was formed in the dark (Figure 8C).

In addition, the UV-Vis absorption measurements of reaction mixture showed a tailing band from 400 to 450 nm (Figure 9A), similar to the absorption curve of B(C₆F₅)₃·H₂O/1aa (Figure 6A). The mixture of 1a and B(C₆F₅)₃·H₂O in THF showed no absorption in visible light region (Figure 9B), different from the result that an Electron Donor-Acceptor (EDA) complex was formed between 1a and anhydrous B(C₆F₅)₃.⁶¹ EPR measurement of the reaction mixture with DMPO showed similar signals (Figure 9D) as those of the mixture of 1a/DMPO/B(C₆F₅)₃·H₂O (Figure 9C), further confirming that the combination of B(C₆F₅)₃·H₂O and 1aa (*in situ* formed from 1a) acts the photocatalyst of the reaction.

Substrate Scope

Under the optimized reaction conditions (See supplemental information), the generality of the reaction was tested by variation of different tetrahydroisoquinolines (Figure 10). All reactions proceeded smoothly to give corresponding products 3 in moderate to good yields. 3aa was obtained in 62% isolated yield in gram scale. Substrate with a β -naphthyl group was compatible with the reaction conditions, and the desired product 3ba could be obtained in 83% yields. For tetrahydroisoquinoline with a hydrogen bond acceptor CN group, the reaction furnished product 3ca in 57% yield. For substrate bearing a Cl atom on the *N*-aryl ring, the reaction delivered 3da in 34% yield. Substrates having electron-donating methoxy substituent were also suitable for this transformation, giving 3ea and 3fa in 66% and 37% yields, respectively. For substrates with a *para*- and *meta*-Me on the *N*-aryl ring, corresponding products 3ga and 3ha were isolated in moderate yields. When substrates had two methoxy groups on the benzene ring (R¹), the reaction could still perform smoothly to give 3ia in 52% yields. To our delight, bupivacaine analogue 3ja could be

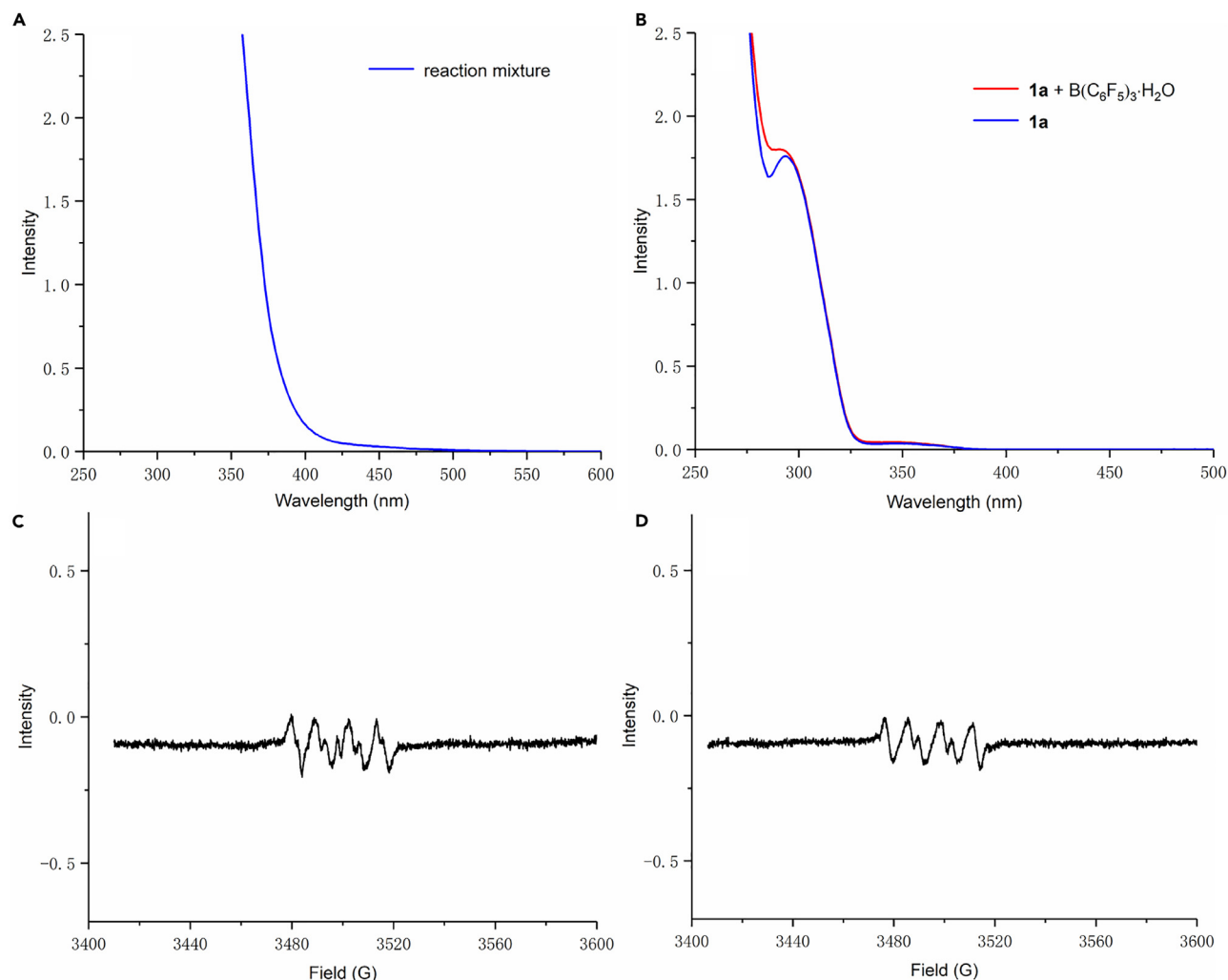


Figure 9. UV-Vis absorption spectra and EPR measurements

(A) **1a**, **2a** and $B(C_6F_5)_3 \cdot H_2O$ (1:1:1) in THF (10^{-3} M) irradiated by blue LEDs for 2 h.
 (B) **1a** in THF (10^{-3} M, blue); **1a** and $B(C_6F_5)_3 \cdot H_2O$ (1:1) in THF (10^{-3} M, red).
 (C) 0.1 mmol **1a**/DMPO and $B(C_6F_5)_3 \cdot H_2O$ (0.01 mmol) THF (1 mL) irradiated by blue LEDs for 30 s.
 (D) 0.1 mmol **1a**/**2a**/DMPO (1:1:1) and $B(C_6F_5)_3 \cdot H_2O$ (0.01 mmol) in THF (1 mL), irradiated by blue LEDs for 30 s.

obtained in 32% yield from *N*-Ph piperidine, and the reaction of *N*-Ph proline also provided corresponding product **3ka** in 39% yield.

Next, a variety of isocyanides were examined and the results are presented in Figure 11. For isocyanide bearing a methoxy group on the benzene ring, the reaction produced the desired product **3ab** in 86% yield. The reactions of electron-deficient aromatic isocyanides provided the corresponding amides **3ac-3ag** in moderate yields. 2-biphenyl isocyanide led to amide product **3ah** in 77% yield. Similarly, for other 2-biaryl substituted isocyanides, products **3ai-3ak** were obtained in moderate to good yields (73%–84%). Aliphatic isocyanides were also suitable for this transformation and gave the desired products **3al-3ar** in 56–90% yields. Notably, ester tethered isocyanide furnished the target product **3as** in 92% yield.

Mechanistic studies

Light on/off experiments were conducted to investigate the effect of light. The mixture of **1a**, **2b** and $B(C_6F_5)_3 \cdot H_2O$ in THF/ H_2O was stirred for 2 h, alternating between 10-min periods of blue LED irradiation and 30 min in the dark. It was noted that the reaction proceeded smoothly on light irradiation, but the

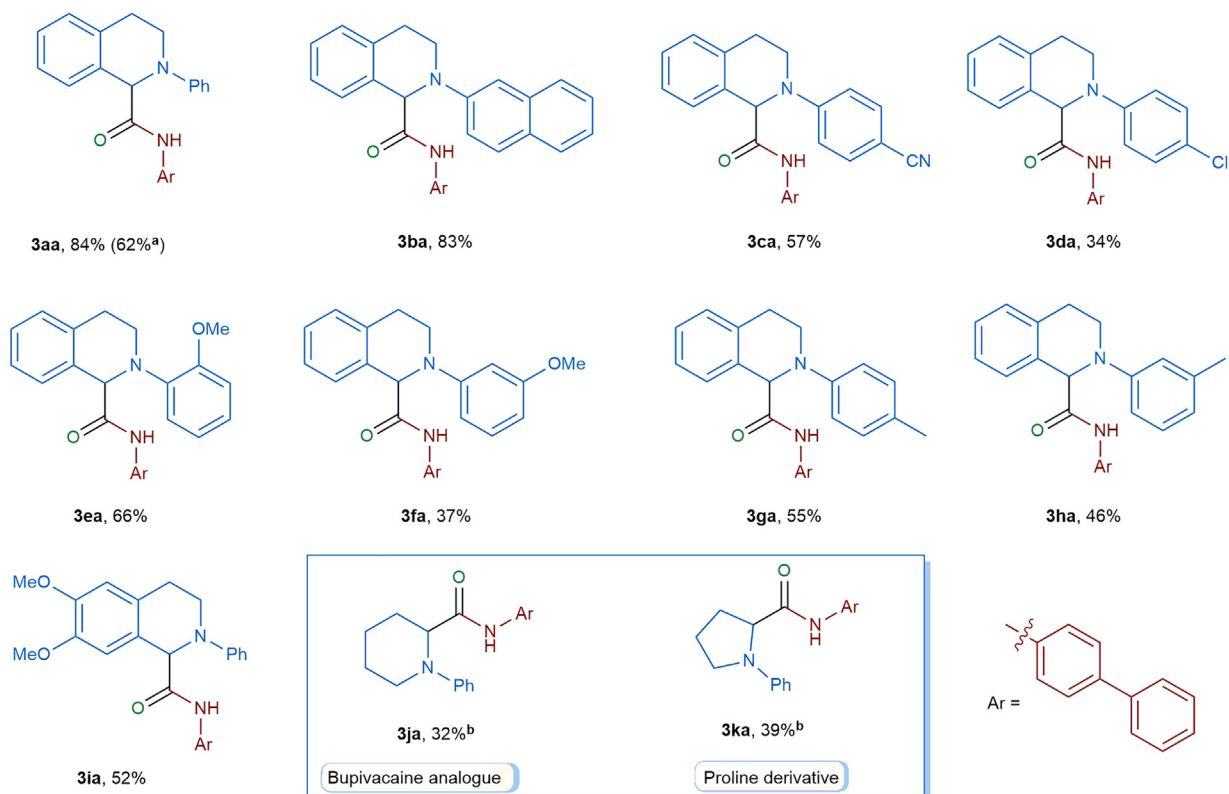
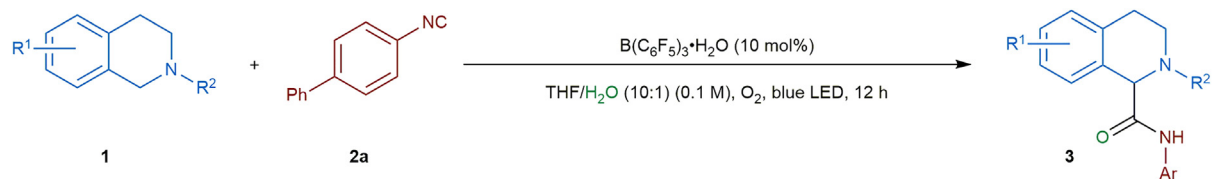


Figure 10. Substrate scope of tetrahydroisoquinolines

Reaction condition: **1** (0.15 mmol), **2a** (0.1 mmol), $B(C_6F_5)_3$ (10 mol %), THF: H_2O = 10: 1 (1 mL), blue LED, O_2 atmosphere at room temperature. a, Gram scale reaction. b, Reaction time: 36 h.

consumption of the isocyanide **2b** immediately stalled without light, indicating that continuous light irradiation is essential for the reaction. (Figure 12).

The reaction mixture was monitored by ^{19}F NMR after completion of the reaction. As shown in Figure 13, the resonance shifts appeared at -135.7 , -160.7 and -165.2 ppm, suggesting that $B(C_6F_5)_3 \cdot H_2O$ is remained after the reaction.⁶² Moreover, potassium iodide-starch test showed discoloration, implying that oxidizing substances were formed in the reaction. Subsequently, H_2O_2 was observed by a reported method using $Ti(SO_4)_2$ as the chromogenic agent, the characteristic peak was monitored at 405 nm (see supplemental information for detail).⁶³

Plausible reaction mechanism

Based on the aforementioned results and reported photoredox aerobic oxidations,^{64–66} a plausible mechanism is proposed (Figure 14). Initially, amide is formed via autoxidation of **1**.⁶⁷ Then, the photocatalyst species PC is formed via hydrogen bond and π - π interactions between $B(C_6F_5)_3 \cdot H_2O$ and amide. In addition, for **1j** and **1k**, *N*-phenyl group of the corresponding amides might take part in the π - π interactions. Next, singlet oxygen (1O_2) is generated via energy transfer (EnT) by excited PC*. Subsequent oxidation of compounds **1** by 1O_2 gives imine cation intermediate, together with the formation of H_2O_2 as a

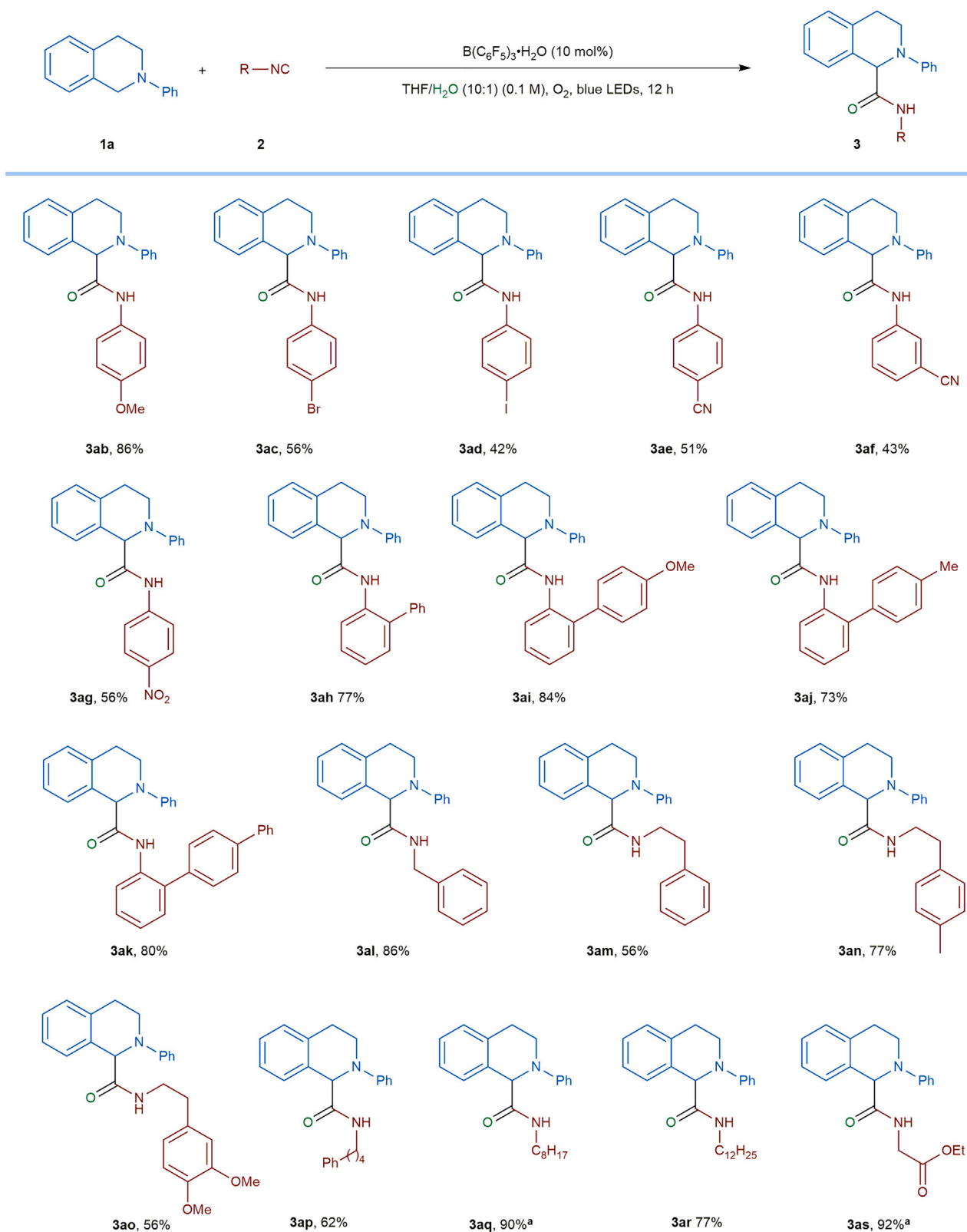


Figure 11. Substrate scope of Isocyanide

Reaction conditions: **1a** (0.1 mmol), **2** (0.15 mmol), $\text{B(C}_6\text{F}_5)_3\cdot\text{H}_2\text{O}$ (10 mol %). a, Reaction time: 14 h.

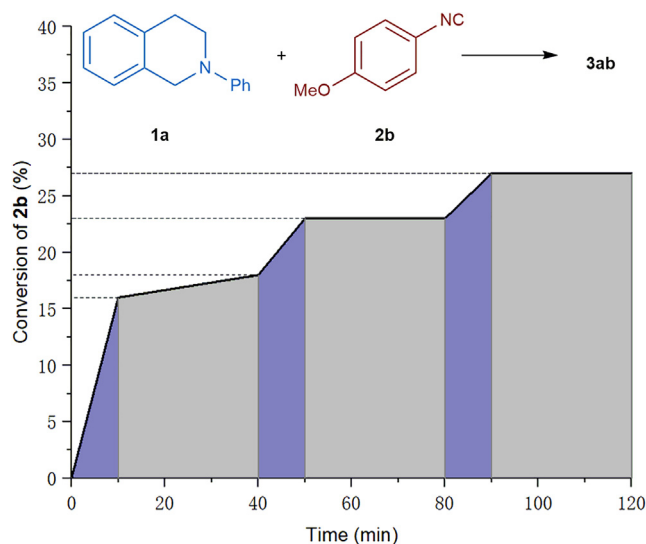


Figure 12. Light on/off experiment

1a (0.15 mmol), **2b** (0.1 mmol), $B(C_6F_5)_3 \cdot H_2O$ (0.01 mmol), THF/ H_2O 10:1, the conversion of **2b** was monitored by GC.

byproduct. Finally, the multiple component reaction occurs between imine cation, isocyanide and H_2O delivers the final products **3**.

Conclusion

In summary, the crystal structure of $B(C_6F_5)_3 \cdot H_2O$ and amide **1aa** was obtained, from which hydrogen bond and π - π interactions are observed. This crystal was composed of six molecules with an eight-membered ring via hydrogen bonds. The boat-chair conformation of the eight-membered ring possesses the lowest energy and the hydrogen bond strength is stronger than normal ones reported in the literature.⁵⁰⁻⁵² Moreover, similar noncovalent interactions were also observed in solution as confirmed by NMR measurements, UV-Vis absorption and fluorescence emission spectra. The π - π interactions demonstrate the specific

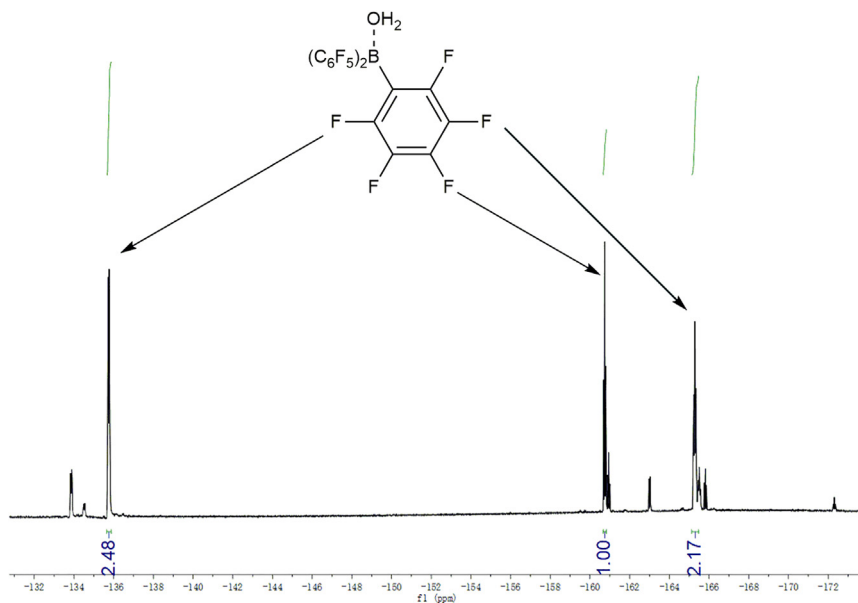


Figure 13. ^{19}F NMR measurement after completion of the reaction

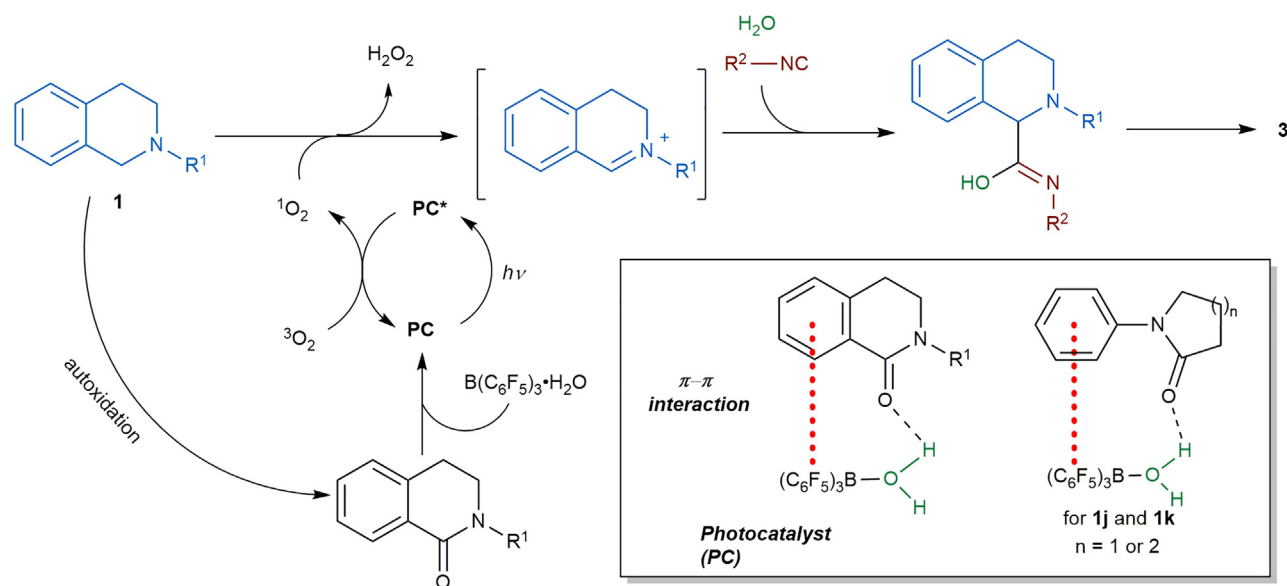


Figure 14. Plausible mechanism

characteristics of $B(C_6F_5)_3 \cdot H_2O$ among other Brønsted acids. Based on the synergistic effect of hydrogen bonds and π - π interactions in $B(C_6F_5)_3 \cdot H_2O$ /amides complex, a photoredox catalysis under visible light is developed using the complex as the photocatalyst.

Limitations of the study

The reaction works well with *N*-aryl tetrahydroisoquinolines; for *N*-alkyl substituted tetrahydroisoquinolines, very low yields were obtained.

STAR★METHODS

Detailed methods are provided in the online version of this paper and include the following:

- KEY RESOURCES TABLE
- RESOURCE AVAILABILITY
 - Lead contact
 - Materials availability
 - Data and code availability
- METHOD DETAILS
 - General information
 - General procedure
 - Spectroscopic data

SUPPLEMENTAL INFORMATION

Supplemental information can be found online at <https://doi.org/10.1016/j.isci.2023.106528>.

ACKNOWLEDGMENTS

We are grateful for the financial support provided by the National Natural Science Foundation of China (22271108, 21871100, 21901079), the Fundamental Research Funds for the Central Universities (2017KFYXJJ166, 2019kfyRCPY096), Huazhong University of Science and Technology (HUST), Hubei Technological Innovation Project (2019ACA125), and the Opening Fund of Hubei Key Laboratory of Bio-inorganic Chemistry and Materia Medica (No. BCMM201805). We also thank the Analytical and Testing Center of HUST, Analytical and Testing Center of the School of Chemistry and Chemical Engineering (HUST) for access to their facilities.

AUTHOR CONTRIBUTIONS

X-Y.T. conceived and supervised the study. S-J.W. performed the syntheses, the spectroscopic characterizations and the X-ray crystal diffraction analysis. S-J.W., L.W., and X-Y.T. analyzed the data and wrote the manuscript.

DECLARATION OF INTERESTS

The authors declare no competing interest.

Received: December 15, 2022

Revised: January 9, 2023

Accepted: March 27, 2023

Published: March 30, 2023

REFERENCES

- Stephan, D.W., and Erker, G. (2010). Frustrated Lewis pairs: metal-free hydrogen activation and more. *Angew. Chem. Int. Ed.* 49, 46–76. <https://doi.org/10.1002/anie.200903708>.
- Stephan, D.W. (2015). Frustrated Lewis pairs: from concept to catalysis. *Acc. Chem. Res.* 48, 306–316. <https://doi.org/10.1021/ar500375j>.
- Stephan, D.W. (2015). Frustrated Lewis pairs. *J. Am. Chem. Soc.* 137, 10018–10032. <https://doi.org/10.1021/jacs.5b06794>.
- Oestreich, M., Hermeke, J., and Mohr, J. (2015). A unified survey of Si-H and H-H bond activation catalysed by electron-deficient boranes. *Chem. Soc. Rev.* 44, 2202–2220. <https://doi.org/10.1039/C4CS00451E>.
- Meng, W., Feng, X., and Du, H. (2018). Frustrated Lewis pairs catalyzed asymmetric metal-free hydrogenations and hydrosilylations. *Acc. Chem. Res.* 51, 191–201. <https://doi.org/10.1021/acs.accounts.7b00530>.
- Basak, S., Winfrey, L., Kustiana, B.A., Melen, R.L., Morrill, L.C., and Pulis, A.P. (2021). Electron deficient borane-mediated hydride abstraction in amines: stoichiometric and catalytic processes. *Chem. Soc. Rev.* 50, 3720–3737. <https://doi.org/10.1039/D0CS00531B>.
- Kumar, G., Roy, S., and Chatterjee, I. (2021). Tris(pentafluorophenyl)borane catalyzed C–C and C–heteroatom bond formation. *Org. Biomol. Chem.* 19, 1230–1267. <https://doi.org/10.1039/D0OB02478c>.
- Welch, G.C., San Juan, R.R., Masuda, J.D., and Stephan, D.W. (2006). Reversible, metal-free hydrogen activation. *Science* 314, 1124–1126. <https://doi.org/10.1126/science.1134230>.
- Parks, D.J., Piers, W.E., Parvez, M., Atencio, R., and Zaworotko, M.J. (1998). Synthesis and solution and solid-state structures of tris(pentafluorophenyl)borane adducts of PhC(O)X (X = H, Me, OEt, NPr₂). *Organometallics* 17, 1369–1377. <https://doi.org/10.1021/om9710327>.
- Mömming, C.M., Otten, E., Kehr, G., Fröhlich, R., Grimme, S., Stephan, D.W., and Erker, G. (2009). Reversible metal-free carbon dioxide binding by frustrated Lewis pairs. *Angew. Chem. Int. Ed.* 48, 6643–6646. <https://doi.org/10.1002/anie.200901636>.
- Otten, E., Neu, R.C., and Stephan, D.W. (2009). Complexation of nitrous oxide by frustrated Lewis pairs. *J. Am. Chem. Soc.* 131, 9918–9919. <https://doi.org/10.1021/ja904377v>.
- Welch, G.C., Coffin, R., Peet, J., and Bazan, G.C. (2009). Band gap control in conjugated oligomers via Lewis acids. *J. Am. Chem. Soc.* 131, 10802–10803. <https://doi.org/10.1021/ja902789w>.
- Sajid, M., Klose, A., Birkmann, B., Liang, L., Schirmer, B., Wiegand, T., Eckert, H., Lough, A.J., Fröhlich, R., Daniliuc, C.G., et al. (2013). Reactions of phosphorus/boron frustrated Lewis pairs with SO₂. *Chem. Sci.* 4, 213–219. <https://doi.org/10.1039/C2SC21161K>.
- Henthorn, J.T., and Agapie, T. (2014). Dioxxygen reactivity with a Ferrocene–Lewis acid pairing: reduction to a boron peroxide in the presence of tris(pentafluorophenyl) borane. *Angew. Chem. Int. Ed.* 53, 12893–12896. <https://doi.org/10.1002/anie.201408462>.
- Hansmann, M.M., López-Andarias, A., Rettenmeier, E., Egler-Lucas, C., Rominger, F., Hashmi, A.S.K., and Romero-Nieto, C. (2016). B(C₆F₅)₃: a Lewis acid that brings the light to the solid state. *Angew. Chem. Int. Ed.* 55, 1196–1199. <https://doi.org/10.1002/anie.201508461>.
- Ye, K.-Y., Kehr, G., Daniliuc, C.G., Liu, L., Grimme, S., and Erker, G. (2016). Coupling of carbon monoxide with nitrogen monoxide at a frustrated Lewis pair template. *Angew. Chem. Int. Ed.* 55, 9216–9219. <https://doi.org/10.1002/anie.201603760>.
- Tao, X., Daniliuc, C.G., Janka, O., Pöttgen, R., Knitsch, R., Hansen, M.R., Eckert, H., Lübbesmeier, M., Studer, A., Kehr, G., and Erker, G. (2017). Reduction of dioxxygen by radical/B(p-C₆F₄X)₃ pairs to give isolable bis(borane)superoxide compounds. *Angew. Chem. Int. Ed.* 56, 16641–16644. <https://doi.org/10.1002/anie.201709309>.
- Antoni, P.W., Golz, C., Holstein, J.J., Pantazis, D.A., and Hansmann, M.M. (2021). Isolation and reactivity of an elusive diazoalkane. *Nat. Chem.* 13, 587–593. <https://doi.org/10.1038/s41557-021-00675-5>.
- Tamke, S., Qu, Z.-W., Sitte, N.A., Flörke, U., Grimme, S., and Paradies, J. (2016). Frustrated Lewis pair-catalyzed cycloisomerization of 1,5-enynes via a 5-endo-dig cyclization/protodeborylation sequence. *Angew. Chem. Int. Ed.* 55, 4336–4339. <https://doi.org/10.1002/anie.201511921>.
- Shang, M., Cao, M., Wang, Q., and Wasa, M. (2017). Enantioselective direct mannich-type reactions catalyzed by frustrated Lewis acid/Brønsted base complexes. *Angew. Chem. Int. Ed.* 56, 13338–13341. <https://doi.org/10.1002/anie.201708103>.
- Zhang, Z.Y., Liu, Z.Y., Guo, R.T., Zhao, Y.Q., Li, X., and Wang, X.C. (2017). B(C₆F₅)₃-Catalyzed ring opening and isomerization of unactivated cyclopropanes. *Angew. Chem. Int. Ed.* 56, 4028–4032. <https://doi.org/10.1002/anie.201700864>.
- Ma, Y., Zhang, L., Luo, Y., Nishiura, M., and Hou, Z. (2017). B(C₆F₅)₃-Catalyzed C–Si/Si–H cross-metathesis of hydrosilanes. *J. Am. Chem. Soc.* 139, 12434–12437. <https://doi.org/10.1021/jacs.7b08053>.
- Shang, M., Chan, J.Z., Cao, M., Chang, Y., Wang, Q., Cook, B., Torker, S., and Wasa, M. (2018). C–H functionalization of amines via alkene-derived nucleophiles through cooperative action of chiral and achiral Lewis acid catalysts: applications in enantioselective synthesis. *J. Am. Chem. Soc.* 140, 10593–10601. <https://doi.org/10.1021/jacs.8b06699>.
- Zhang, J., Park, S., and Chang, S. (2018). Catalytic access to bridged sila-N-heterocycles from piperidines via cascade sp³ and sp² C–Si bond formation. *J. Am. Chem. Soc.* 140, 13209–13213. <https://doi.org/10.1021/jacs.8b08733>.
- Han, Y., Zhang, S., He, J., and Zhang, Y. (2017). B(C₆F₅)₃-Catalyzed (convergent) disproportionation reaction of indoles. *J. Am. Chem. Soc.* 139, 7399–7407. <https://doi.org/10.1021/jacs.7b03534>.

26. Cabré, A., Rafael, S., Sciortino, G., Ujaque, G., Verdaguier, X., Lledós, A., and Riera, A. (2020). Catalytic regioselective isomerization of 2,2-disubstituted oxetanes to homoallylic alcohols. *Angew. Chem. Int. Ed.* **59**, 7521–7527. <https://doi.org/10.1002/anie.201915772>.
27. Arslan, M., Kiskan, B., and Yagci, Y. (2018). Ring-opening polymerization of 1,3-benzoxazines via borane catalyst. *Polymers* **10**, 239. <https://doi.org/10.3390/polym10030239>.
28. Hatano, M., Sakamoto, T., Mochizuki, T., and Ishihara, K. (2019). Tris(pentafluorophenyl) borane-Assisted chiral phosphoric acid catalysts for Enantioselective Inverse-electron-demand hetero-diels-alder reaction of α,β -substituted acroleins. *Asian J. Org. Chem.* **8**, 1061–1066. <https://doi.org/10.1002/ajoc.201900104>.
29. Retini, M., Bartolucci, S., Bartocchini, F., Mari, M., and Piersanti, G. (2019). Concise and convergent enantioselective total syntheses of (+)- and (-)-Fumimycin. *J. Org. Chem.* **84**, 12221–12227. <https://doi.org/10.1021/acs.joc.9b02020>.
30. Cai, L., Liu, X., Wang, J., Chen, L., Li, X., and Cheng, J.-P. (2020). Enantioselective and regioselective aza-Friedel-Crafts reaction of electron-rich phenols with isatinderived ketimines. *Chem. Commun.* **56**, 10361–10364. <https://doi.org/10.1039/D0CC04966B>.
31. Ishihara, H., Huang, J., Mochizuki, T., Hatano, M., and Ishihara, K. (2021). Enantio- and diastereoselective carbonyl-Ene cyclization-acetalization tandem reaction catalyzed by tris(pentafluorophenyl)borane-assisted chiral phosphoric acids. *ACS Catal.* **11**, 6121–6127. <https://doi.org/10.1021/acscatal.1c01242>.
32. Meng, S.-S., Tang, X., Luo, X., Wu, R., Zhao, J.-L., and Chan, A.S.C. (2019). Borane-catalyzed chemoselectivity-controllable N-alkylation and *ortho* C-alkylation of unprotected arylamines using benzylic alcohols. *ACS Catal.* **9**, 8397–8403. <https://doi.org/10.1021/acscatal.9b03038>.
33. Chen, X., Patel, K., and Marek, I. (2023). Stereoselective construction of tertiary homoallyl alcohols and ethers by nucleophilic substitution at quaternary carbon stereocenter. *Angew. Chem. Int. Ed.* **62**, e202212425. <https://doi.org/10.1002/anie.202212425>.
34. Mahdi, T., and Stephan, D.W. (2014). Enabling catalytic ketone hydrogenation by frustrated Lewis pairs. *J. Am. Chem. Soc.* **136**, 15809–15812. <https://doi.org/10.1021/ja508829x>.
35. Gyömöre, Á., Bakos, M., Földes, T., Pápai, I., Domján, A., and Soós, T. (2015). Moisture-tolerant frustrated Lewis pair catalyst for hydrogenation of aldehydes and ketones. *ACS Catal.* **5**, 5366–5372. <https://doi.org/10.1021/acscatal.5b01299>.
36. Scott, D.J., Simmons, T.R., Lawrence, E.J., Wildgoose, G.G., Fuchter, M.J., and Ashley, A.E. (2015). Facile protocol for water-tolerant “frustrated Lewis pair”-catalyzed hydrogenation. *ACS Catal.* **5**, 5540–5544. <https://doi.org/10.1021/acscatal.5b01417>.
37. Fasano, V., Radcliffe, J.E., and Ingleson, M.J. (2016). B(C₆F₅)₃-Catalyzed reductive amination using hydrosilanes. *ACS Catal.* **6**, 1793–1798. <https://doi.org/10.1021/acscatal.5b02896>.
38. Bergquist, C., Bridgewater, B.M., Harlan, C.J., Norton, J.R., Friesner, R.A., and Parkin, G. (2000). Aqua, alcohol, and acetonitrile adducts of tris(perfluorophenyl)borane: evaluation of Bronsted acidity and ligand lability with experimental and computational methods. *J. Am. Chem. Soc.* **122**, 10581–10590. <https://doi.org/10.1021/ja001915g>.
39. Danopoulos, A.A., Galsworthy, J.R., Green, M.L.H., Doerrer, L.H., Cafferkey, S., and Hursthouse, M.B. (1998). Equilibria in the B(C₆F₅)₃-H₂O system: synthesis and crystal structures of H₂O·B(C₆F₅)₃ and the anions [HOB(C₆F₅)₃]⁻ and [(F₅C₆)₃B(μ-OH)B(C₆F₅)₃]⁻. *Chem. Commun.* 2529–2560. <https://doi.org/10.1039/A804918A>.
40. Focante, F., Camurati, I., Resconi, L., Guidotti, S., Beringhelli, T., D’Alfonso, G., Donghi, D., Maggioni, D., Mercandelli, P., and Sironi, A. (2006). Synthesis and reactivity of N-heterocycle-B(C₆F₅)₃ complexes. 4. Competition between pyridine- and pyrrole-type substrates toward B(C₆F₅)₃: structure and dynamics of 7-B(C₆F₅)₃-7-azaindole and [7-Azaindolium]⁺[HOB(C₆F₅)₃]⁻. *Inorg. Chem.* **45**, 1683–1692. <https://doi.org/10.1021/ic051285p>.
41. Dryzhakov, M., Hellal, M., Wolf, E., Falk, F.C., and Moran, J. (2015). Nitro-assisted bronsted acid catalysis: application to a challenging catalytic azidation. *J. Am. Chem. Soc.* **137**, 9555–9558. <https://doi.org/10.1021/jacs.5b06055>.
42. Dryzhakov, M., and Moran, J. (2016). Autocatalytic friedel-crafts reactions of tertiary aliphatic fluorides initiated by B(C₆F₅)₃·H₂O. *ACS Catal.* **6**, 3670–3673. <https://doi.org/10.1021/acscatal.6b00866>.
43. Dryzhakov, M., Richmond, E., Li, G., and Moran, J. (2017). Catalytic B(C₆F₅)₃·H₂O-promoted defluorinative functionalization of tertiary aliphatic fluorides. *J. Fluor. Chem.* **193**, 45–51. <https://doi.org/10.1016/j.jfluchem.2016.11.005>.
44. Shibuya, M., Okamoto, M., Fujita, S., Abe, M., and Yamamoto, Y. (2018). Boron-catalyzed double hydrofunctionalization reactions of unactivated alkynes. *ACS Catal.* **8**, 4189–4193. <https://doi.org/10.1021/acscatal.8b00955>.
45. San, H.H., Wang, S.-J., Jiang, M., and Tang, X.-Y. (2018). Boron-catalyzed O–H bond insertion of α -aryl α -diazoesters in water. *Org. Lett.* **20**, 4672–4676. <https://doi.org/10.1021/acs.orglett.8b01988>.
46. Bennett, C.K., Bhagat, M.N., Zhu, Y., Yu, Y., Raghuraman, A., Belowich, M.E., Nguyen, S.T., Notestein, J.M., and Broadbelt, L.J. (2019). Strong influence of the nucleophile on the rate and selectivity of 1,2-epoxyoctane ring opening catalyzed by tris(pentafluorophenyl)borane, B(C₆F₅)₃. *ACS Catal.* **9**, 11589–11602. <https://doi.org/10.1021/acscatal.9b02607>.
47. Bhagat, M.N., Chang, G.-F., Bennett, C.K., Raghuraman, A., Belowich, M.E., Broadbelt, L.J., Nguyen, S.T., and Notestein, J.M. (2022). Improving and stabilizing fluorinated aryl borane catalysts for epoxide ring-opening. *Applied Catalysis A, General* **636**, 118601. <https://doi.org/10.1016/j.apcata.2022.118601>.
48. Bock, C.W., Trachtman, M., and George, P. (1981). An ab initio study of the influence of substituents and intramolecular hydrogen bonding on the carbonyl bond length and stretching force constant. I. Monosubstituted carbonyl compounds. *J. Comput. Chem.* **2**, 30–37. <https://doi.org/10.1002/jcc.540020107>.
49. Lynch, D.E., and Reeves, C.R. (2019). Statistical analysis of the effect of a single OH hydrogen-bonding interaction on carbonyl bond lengths. *J. Mol. Struct.* **1180**, 158–162. <https://doi.org/10.1016/j.molstruc.2018.11.100>.
50. Janiak, C. (2000). A critical account on π - π stacking in metal complexes with aromatic nitrogen-containing ligands. *J. Chem. Soc., Dalton Trans.* 3885–3896. <https://doi.org/10.1039/B003010O>.
51. Hendrickson, J.B. (1967). Molecular geometry. V. Evaluation of functions and conformations of medium rings. *J. Am. Chem. Soc.* **89**, 7036–7043. <https://doi.org/10.1021/ja01002a036>.
52. Hu, Y.-J., Li, L.-X., Han, J.-C., Min, L., and Li, C.-C. (2020). Recent advances in the total synthesis of natural products containing eight-membered carbocycles (2009–2019). *Chem. Rev.* **120**, 5910–5953. <https://doi.org/10.1021/acs.chemrev.0c00045>.
53. Gilli, P., Pretto, L., Bertolasi, V., and Gilli, G. (2009). Predicting hydrogen-bond strengths from Acid–Base molecular properties. The pK_s slide rule: toward the solution of a long-lasting problem. *Acc. Chem. Res.* **42**, 33–44. <https://doi.org/10.1021/ar800001k>.
54. Buldashov, I.A., Medvedev, A.G., Mikhaylov, A.A., Churakov, A.V., Lev, O., and Prikhodchenko, P.V. (2022). Non-covalent interactions of the hydroperoxo group in crystalline adducts of organic hydroperoxides and their potassium salts. *CrystEngComm* **24**, 6101–6108. <https://doi.org/10.1039/D2CE01017H>.
55. Shetty, A.S., Zhang, J., and Moore, J.S. (1996). Aromatic π -stacking in solution as revealed through the aggregation of Phenylacetylene macrocycles. *J. Am. Chem. Soc.* **118**, 1019–1027. <https://doi.org/10.1021/ja9528893>.
56. Viglianti, L., Leung, N.L.C., Xie, N., Gu, X., Sung, H.H.Y., Miao, Q., Williams, I.D., Licandro, E., and Tang, B.Z. (2017). Aggregation-induced emission: mechanistic study of the clusteroluminescence of tetrathienylethene. *Chem. Sci.* **8**, 2629–2639. <https://doi.org/10.1039/C6SC05192H>.
57. Harbour, J.R., and Hair, M.L. (1978). Detection of superoxide ions in nonaqueous media.

- Generation by photolysis of pigment dispersions. *J. Phys. Chem.* **82**, 1397–1399. <https://doi.org/10.1021/j100501a015>.
58. Buettner, G.R. (1987). Spin Trapping: ESR parameters of spin adducts. *Free Radic. Biol. Med.* **3**, 259–303. [https://doi.org/10.1016/S0891-5849\(87\)80033-3](https://doi.org/10.1016/S0891-5849(87)80033-3).
59. Gray, B., and Carmichael, A.J. (1992). Kinetics of superoxide scavenging by dismutase enzymes and manganese mimics determined by electron spin resonance. *Biochem. J.* **281**, 795–802. <https://doi.org/10.1042/bj2810795>.
60. Weng, M., Zhang, M., and Shen, T. (1997). EPR studies of the photodynamic action of mercapto-substituted hypocrellin B derivatives: formation of semiquinone radical anion and activated oxygen on illumination with visible light. *J. Photochem. Photobiol., A: Chem* **108**, 159–167. [https://doi.org/10.1016/S1010-6030\(97\)00072-5](https://doi.org/10.1016/S1010-6030(97)00072-5).
61. Aramaki, Y., Imaizumi, N., Hotta, M., Kumagai, J., and Ooi, T. (2020). Exploiting single-electron transfer in Lewis pairs for catalytic bond-forming reactions. *Chem. Sci.* **11**, 4305–4311. <https://doi.org/10.1039/D0SC01159B>.
62. Beringhelli, T., Maggioni, D., and D'Alfonso, G. (2001). ^1H and ^{19}F NMR investigation of the reaction of $\text{B}(\text{C}_6\text{F}_5)_3$ with water in toluene solution. *Organometallics* **20**, 4927–4938. <https://doi.org/10.1021/om010610n>.
63. Xu, M., Bunes, B.R., and Zang, L. (2011). Paper-based vapor detection of hydrogen peroxide: colorimetric sensing with tunable interface. *ACS Appl. Mater. Interfaces* **3**, 642–647. <https://doi.org/10.1021/am1012535>.
64. Ugi, I. (2001). Recent progress in the chemistry of multicomponent reactions. *Pure Appl. Chem.* **73**, 187–191. <https://doi.org/10.1351/pac200173010187>.
65. Gligorovski, S., Strekowski, R., Barbati, S., and Vione, D. (2015). Environmental implications of hydroxyl radicals ($\cdot\text{OH}$). *Chem. Rev.* **115**, 13051–13092. <https://doi.org/10.1021/cr500310b>.
66. Wang, D., Weinstein, A.B., White, P.B., and Stahl, S.S. (2018). Ligand-Promoted palladium-catalyzed aerobic oxidation reactions. *Chem. Rev.* **118**, 2636–2679. <https://doi.org/10.1021/acs.chemrev.7b00334>.
67. Thapa, P., Corral, E., Sardar, S., Pierce, B.S., and Foss, F.W. (2019). Isoindolinone synthesis: selective dioxane-mediated aerobic oxidation of isoindolines. *J. Org. Chem.* **84**, 1025–1034. <https://doi.org/10.1021/acs.joc.8b01920>.

STAR★METHODS

KEY RESOURCES TABLE

REAGENT or RESOURCE	SOURCE	IDENTIFIER
Chemicals, peptides, and recombinant proteins		
1,2,3,4-Tetrahydro-2-isoquinoline	Meryer	CAS: 91-21-4
1,2,3,4-tetrahydro-6,7-dimethoxy-isoquinolin	Meryer	CAS: 1745-07-9
4-Aminobiphenyl	Meryer	CAS: 92-67-1
4-Chlorobromobenzene	Energy Chemical	CAS: 106-39-8
4-Bromobenzonitrile	Energy Chemical	CAS: 623-00-7
2-Bromoanisole	Energy Chemical	CAS: 578-57-4
4-Bromoanisole	Adamas	CAS: 104-92-7
3-Bromoanisole	Adamas	CAS: 2398-37-0
4-Bromotoluene	Adamas	CAS: 106-38-7
3-Bromotoluene	Adamas	CAS: 591-17-3
4-Bromoaniline	Adamas	CAS: 106-40-1
4-Iodoaniline	Adamas	CAS: 540-37-4
<i>p</i> -Anisidine	Adamas	CAS: 104-94-9
4-Aminobenzonitrile	Adamas	CAS: 873-74-5
4-Nitroaniline	Adamas	CAS: 100-01-6
2-Aminobiphenyl	Adamas	CAS: 90-41-5
4'-Methyl-Bpphenyl-2-ylamine	Adamas	CAS: 1204-43-9
4'-Methoxy-Bpphenyl-2-ylamine	Adamas	CAS: 38089-03-1
Deposited data		
Complex of B(C ₆ F ₅) ₃ ·H ₂ O and amide 1aa.	CCDC	CCDC-2207426
Other		
Silica gel (200-300 mesh)	Huanghai	https://www.aladdin-e.com/
AVIII 400 MHz	Bruker	https://www.bruker.com

RESOURCE AVAILABILITY

Lead contact

Further information and requests for resources should be directed to and will be fulfilled by the lead contact, Xiang-Ying Tang (xtang@hust.edu.cn).

Materials availability

All materials generated in this study are available within the article and the [supplemental information](#) or from the [lead contact](#) upon reasonable request.

Data and code availability

- The original crystal structure of B(C₆F₅)₃·H₂O with 1aa has been deposited at CCDC and is publicly available as of the date of publication. CCDC number is listed in the [key resources table](#).
- This paper does not report original code.
- Any additional information required to reanalyze the data reported in this paper can be obtained from the [lead contact](#) upon request.

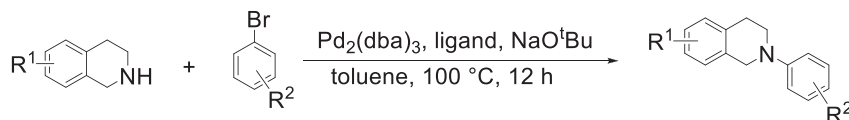
METHOD DETAILS

General information

The nuclear magnetic resonance spectra were recorded on the Bruker Avance III 400 MHz with tetramethylsilane (TMS) as an internal standard. High resolution mass spectra were recorded using analyses by BrukerDaltonics SolariX 7.0T. Organic solvents used were dried by standard methods when necessary. Commercially obtained reagents were used without further purification. Flash column chromatography was performed using 300-400 mesh silica gel. For thin-layer chromatography (TLC), silica gel plates (Huanghai GF254) were used. EPR (electron paramagnetic resonance) spectra were recorded by Bruker EMXmicro-6/1 instrument. X-Ray diffraction were collected by XtaLAB PRO MM007HF Cu (Rigaku, Japan). UV-vis spectra were obtained on a UV-2600 (Shimadzu). Fluorescence spectroscopic studies were performed with a RF-5301PC (Shimadzu). All heat sources are oil bath. All light sources are 3 W blue LED bands and the wavelength of peak is 427 nm. The distance from the light source to the container is 3-5 cm.

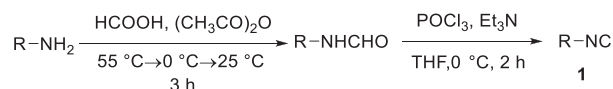
General procedure

Synthesis of substrate isoquinolines



A mixture of Pd₂(dba)₃ (3 mol%) and ligand (2-Dicyclohexylphosphino-2',6'-dimethoxybiphenyl) (8 mol%) were placed into an oven dried reaction tube. Subsequently, the reaction tube was degassed with N₂ for three times. Then, dry toluene, bromoarene (1.0 equiv.), 1,2,3,4-tetrahydroisoquinoline (1.2 equiv.) and ^tBuONa (1.4 equiv.) were sequentially added under nitrogen protection. Then the reaction mixture was heated to 100 °C for 12 h. After completion, the resulting reaction mixture was slowly cooled to room temperature, quenched by brine and extracted with ethylacetate. The organic layer was dried over Na₂SO₄ and concentrated under reduced pressure. The crude product was purified by column chromatography on silica gel. In addition, **1a-1h** are known compound.

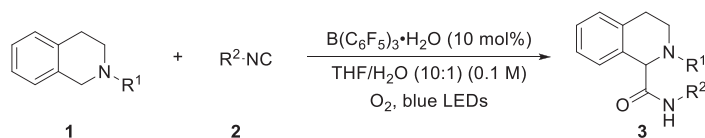
Synthesis of isocyanides



A mixture of HCOOH (2.0 equiv) and (CH₃CO)₂O (2.0 equiv.) were stirred at 55 °C for 2 h. Before aniline (1.0 equiv.) was added the reaction mixture was cooled down at 0 °C, then continued stirring for 2 h at room temperature. After consumption of aniline, all the volatiles were removed under reduced pressure and the crude product was directly used in the next step without further purification.

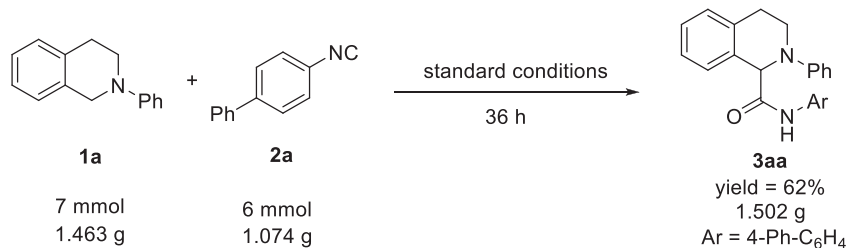
To a stirred solution of crude product in dry THF at 0 °C were added Et₃N (5.0 equiv.) and POCl₃ (1.2 equiv.) dropwise sequentially. After stirring for 2 h at 0 °C, the reaction was quenched with water and extracted with ethylacetate (EA) for three times. The organic layer was washed with brine and dried over anhydrous Na₂SO₄ and concentrated under reduced pressure. The crude product was purified by column chromatography on silica gel to observed pure product **2**. In addition, **2a-2s** are known compound.

Synthesis of compounds 3



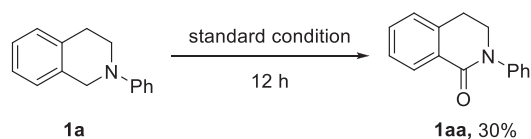
To a stirred solution of **1** (0.15 mmol, 1.5 equiv.) in mixed solvent (1 mL, THF: H₂O = 10:1) were added **2** (0.1 mmol, 1.0 equiv.) and boron catalyst (10 mol%). The resulting solution was stirred in the presence of O₂ under blue light irradiation. The reaction was monitored by TLC, the crude products were purified by flash column chromatography to provide a series of amide compounds **3**. In addition, **3aa** was known compound.

Gram scale reaction



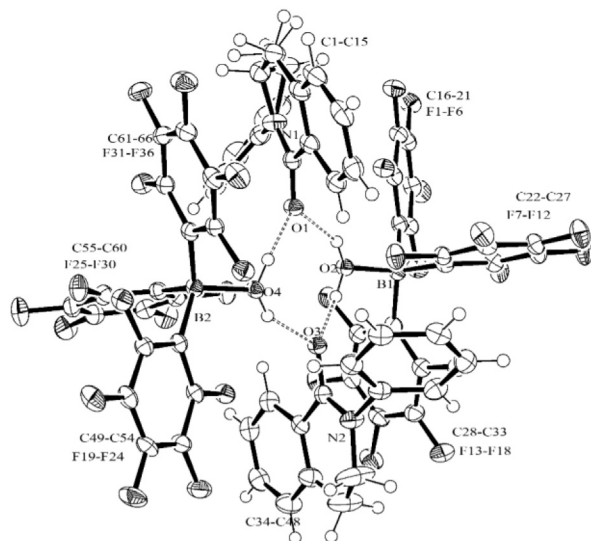
To a stirred solution of **2a** (6 mmol, 1.074 g) in mixed solvent (50 mL, THF: H₂O = 10:1) were added to **1a** (7 mmol, 1.463 g) and boron catalyst (10 mol%, 0.307 g). The resulting solution was stirred at blue LED and O₂ for 36 h. The crude product was purified by flash column chromatography to provide a series of amide compound **3aa** (1.502 g, 62%).

Oxidation reaction of 1a



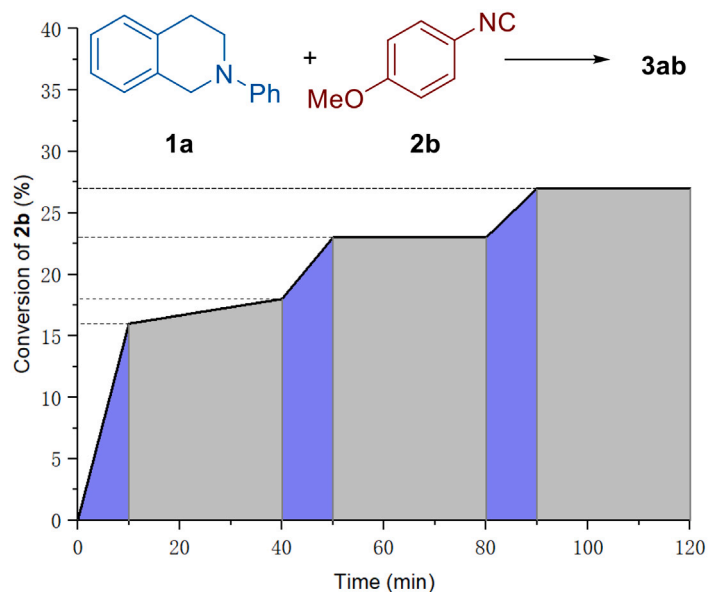
To a stirred solution of **1a** (0.1 mmol, 20.9 mg, 1.0 equiv.) in mixed solvent (1 mL, THF: H₂O = 10:1) was added to boron catalyst (10 mol%). The resulting solution was stirred at blue LEDs and 1 atm O₂ for 12 h. The crude product was purified by flash column chromatography to provide **1aa** (6.6 mg, 30%) and **1a** (12.7 mg, 61%).

X-ray crystal structure analysis for 1aa



X-ray crystal structure analysis of **C1**. A clear colorless plate. Formula $C_{33}H_{15}BF_{15}NO_2$, $M = 753.27$, $0.25 \times 0.2 \times 0.05$ mm, $a = 12.0787(1)$, $b = 11.9169(1)$, $c = 41.6237(3)$ Å, $\beta = 97.510(1)^\circ$, $V = 5939.95(8)$ Å³, $\mu = 1.518$ mm⁻¹, $0.651 \leq T \leq 1.000$, $\Theta(\text{max}) = 74.296^\circ$, $R = 0.0381$, $wR^2 = 0.1036$, temperature = 293 K, hydrogen atoms calculated and refined as riding atoms.

Light on/off experiments



To a stirred solution of the 1-isocyanato-4-methoxybenzene (**2b**, 0.1 mmol, 1.0 equiv.) and boron catalyst (10 mol%) in mixed solvent (1mL, THF: H₂O = 10:1) was added the N-phenyl-1,2,3,4-tetrahydroisoquinoline (**1a**, 0.15 mmol, 1.5 equiv.). Besides, 0.1 mmol dodecane was added as internal

standard. The light was kept on for ten minutes then kept off for thirty minutes. The reaction mixture 0.05 mL was taken and diluted with 1,2-dichloroethane (DCE) to 2 mL for gas chromatography (GC) monitoring.

Spectroscopic data

N-([1,1'-biphenyl]-4-yl)-2-phenyl-1,2,3,4-tetrahydroisoquinoline-1-carboxamide (3aa)

Purified by silica gel chromatography (petroleum ether/ethyl acetate 10:1 as the eluent). White solid (33.7 mg, 84% yield). m.p.: 192–194 °C. ¹H NMR (400 MHz, CDCl₃, TMS) δ 8.88 (s, 1H), 7.65 (d, *J* = 6.8 Hz, 1H), 7.57–7.49 (m, 6H), 7.36–7.27 (m, 4H), 7.26–7.23 (m, 1H), 7.18 (d, *J* = 7.2 Hz, 1H), 7.02 (d, *J* = 8.0 Hz, 2H), 6.95 (dd, *J*₁ = *J*₂ = 7.6 Hz, 1H), 5.09 (s, 1H), 3.94 (dt, *J* = 9.6 Hz, *J* = 4.4 Hz, 1H), 3.40 (td, *J* = 10.8 Hz, *J* = 4.0 Hz, 1H), 3.16–3.00 (m, 2H). ¹³C{¹H} NMR (100 MHz, CDCl₃, TMS) δ 170.6, 149.4, 140.5, 137.3, 136.7, 134.5, 132.1, 129.6, 129.1, 127.8, 127.7, 127.5, 127.1, 126.9, 120.4, 120.1, 115.3, 66.5, 45.4, 28.8. IR ν 3298, 3034, 2251, 2228, 1662, 1287, 858, 690 cm⁻¹. HRMS (ESI) *m/z*: calcd for C₂₈H₂₅N₂O [M+H]⁺ 405.1961; found 405.1960.

N-([1,1'-biphenyl]-4-yl)-2-(naphthalen-2-yl)-1,2,3,4-tetrahydroisoquinoline-1-carboxamide (3ba)

Purified by silica gel chromatography (petroleum ether/ethyl acetate 10:1 as the eluent). White solid (37.6 mg, 83% yield). m.p.: 141–143 °C. ¹H NMR (400 MHz, CDCl₃, TMS) δ 8.89 (s, 1H), 7.79 (d, *J* = 8.8 Hz, 1H), 7.75–7.67 (m, 3H), 7.54–7.45 (m, 6H), 7.44–7.35 (m, 3H), 7.33–7.24 (m, 6H), 7.17 (d, *J* = 7.2 Hz, 1H), 5.24 (s, 1H), 4.03 (dt, *J* = 10.8 Hz, *J* = 4.0 Hz, 1H), 3.50 (td, *J* = 10.8 Hz, *J* = 4.0 Hz, 1H), 3.18–3.01 (m, 2H). ¹³C{¹H} NMR (100 MHz, CDCl₃, TMS) δ 147.0, 140.5, 137.4, 136.7, 134.5, 134.4, 132.0, 129.5, 129.2, 128.8, 128.6, 127.9, 127.8, 127.6, 127.5, 127.1, 126.94, 126.9, 126.8, 126.7, 123.9, 120.1, 117.5, 66.2, 45.9, 28.8. IR ν 3303, 3052, 2924, 1667, 1596, 1386, 1112, 834 cm⁻¹. HRMS (ESI) *m/z*: calcd for C₃₂H₂₇N₂O [M+H]⁺ 455.2118; found 455.2117.

N-([1,1'-biphenyl]-4-yl)-2-(4-cyanophenyl)-1,2,3,4-tetrahydroisoquinoline-1-carboxamide (3ca)

Purified by silica gel chromatography (petroleum ether/ethyl acetate 10:1 as the eluent). White solid (24.5 mg, 57% yield). m.p.: 137–139 °C. ¹H NMR (400 MHz, CDCl₃, TMS) δ 8.37 (s, 1H), 7.61–7.58 (m, 1H), 7.55–7.48 (m, 8H), 7.40 (dd, *J*₁ = *J*₂ = 8.0 Hz, 2H), 7.33–7.28 (m, 3H), 7.23–7.20 (m, 1H), 6.95 (d, *J* = 8.8 Hz, 2H), 5.18 (s, 1H), 4.06–4.00 (m, 1H), 3.43 (td, *J* = 11.2 Hz, *J* = 3.6 Hz, 1H), 3.25–3.16 (m, 1H), 3.07 (dt, *J* = 15.6 Hz, *J* = 3.6 Hz, 1H). ¹³C{¹H} NMR (100 MHz, CDCl₃, TMS) δ 169.4, 152.0, 140.3, 137.8, 136.3, 134.4, 133.8, 131.7, 128.8, 128.4, 127.8, 127.6, 127.3, 127.27, 126.9, 120.4, 119.8, 113.7, 101.5, 65.6, 44.5, 28.7. IR ν 3319, 3026, 2831, 2246, 1662, 1318, 904, 722 cm⁻¹. HRMS (ESI) *m/z*: calcd for C₂₉H₂₄N₃O [M+H]⁺ 430.1914; found 430.1907.

N-([1,1'-biphenyl]-4-yl)-2-(4-chlorophenyl)-1,2,3,4-tetrahydroisoquinoline-1-carboxamide (3da)

Purified by silica gel chromatography (petroleum ether/ethyl acetate 10:1 as the eluent). White solid (14.9 mg, 34% yield). m.p.: 188–190 °C. ¹H NMR (400 MHz, CDCl₃, TMS) δ 8.72 (s, 1H), 7.63 (d, *J* = 6.8 Hz, 1H), 7.55–7.48 (m, 6H), 7.42–7.37 (m, 2H), 7.33–7.24 (m, 5H), 7.17 (d, *J* = 6.8 Hz, 1H), 6.92 (d, *J* = 9.2 Hz, 2H), 5.03 (s, 1H), 3.94–3.88 (m, 1H), 3.35 (td, *J* = 10.8 Hz, *J* = 3.6 Hz, 1H), 3.16–3.08 (m, 1H), 3.01 (dt, *J* = 12.0 Hz, *J* = 3.2 Hz, 1H). ¹³C{¹H} NMR (100 MHz, CDCl₃, TMS) δ 170.2, 148.0, 140.4, 137.5, 136.6, 134.3, 131.8, 129.4, 129.0, 128.8, 127.9, 127.8, 127.6, 127.2, 127.0, 126.9, 125.5, 120.1, 116.4, 66.4, 45.6, 28.8. IR ν 3255, 3061, 2920, 2851, 1596, 1331, 1052, 840 cm⁻¹. HRMS (ESI) *m/z*: calcd for C₂₈H₂₄N₂OCl [M+H]⁺ 439.1572; found 439.1571.

N-([1,1'-biphenyl]-4-yl)-2-(2-methoxyphenyl)-1,2,3,4-tetrahydroisoquinoline-1-carboxamide (3ea)

Purified by silica gel chromatography (petroleum ether/ethyl acetate 10:1 as the eluent). White solid (28.6 mg, 66% yield). m.p.: 66–68 °C. ¹H NMR (400 MHz, CDCl₃, TMS) δ 9.98 (s, 1H), 7.72 (d, *J* = 7.2 Hz, 1H), 7.60–7.50 (m, 6H), 7.40 (dd, *J*₁ = *J*₂ = 7.6 Hz, 2H), 7.32–7.22 (m, 3H), 7.17–7.10 (m, 3H), 6.97–6.87 (m, 2H), 5.08 (s, 1H), 4.00 (s, 3H), 3.48–3.31 (m, 2H), 3.03–2.84 (m, 2H). ¹³C{¹H} NMR (100 MHz, CDCl₃, TMS) δ 170.5, 153.8, 140.6, 139.0, 137.6, 136.6, 134.6, 132.1, 129.0, 128.7, 128.6, 127.5, 127.2, 127.0, 126.8, 126.2, 125.6, 123.3, 121.3, 119.5, 111.5, 65.2, 55.6, 47.7, 28.0. IR ν 3298, 3026, 2849, 2228, 1490, 1035, 904, 720 cm⁻¹. HRMS (ESI) *m/z*: calcd for C₂₉H₂₇N₂O₂[M+H]⁺ 435.2067; found 435.2066.

***N*-([1,1'-biphenyl]-4-yl)-2-(3-methoxyphenyl)-1,2,3,4-tetrahydroisoquinoline-1-carboxamide (3fa)**

Purified by silica gel chromatography (petroleum ether/ethyl acetate 10:1 as the eluent). White solid (16.1 mg, 37% yield). m.p.: 64–66°C. ¹H NMR (400 MHz, CDCl₃, TMS) δ 8.81 (s, 1H), 7.63 (d, *J* = 7.2 Hz, 1H), 7.57–7.48 (m, 6H), 7.42–7.38 (m, 2H), 7.33–7.21 (m, 4H), 7.17 (d, *J* = 6.8 Hz, 1H), 6.62–6.56 (m, 2H), 5.10 (s, 1H), 3.95–3.89 (m, 1H), 3.80 (s, 3H), 3.39 (td, *J* = 10.8 Hz, *J* = 4.0 Hz, 1H), 3.15–2.99 (m, 2H). ¹³C{¹H} NMR (100 MHz, CDCl₃, TMS) δ 170.4, 160.8, 150.8, 140.5, 137.3, 136.7, 134.5, 132.1, 130.3, 129.1, 128.8, 127.7, 127.5, 127.1, 126.8, 120.1, 108.0, 105.0, 101.9, 66.4, 55.3, 45.3, 28.8. IR ν 3319, 3025, 2920, 2847, 1662, 1445, 1166, 757 cm⁻¹. HRMS (ESI) *m/z*: calcd for C₂₉H₂₇N₂O₂[M+H]⁺ 435.2067; found 435.2066.

***N*-([1,1'-biphenyl]-4-yl)-2-(*p*-tolyl)-1,2,3,4-tetrahydroisoquinoline-1-carboxamide (3ga)**

Purified by silica gel chromatography (petroleum ether/ethyl acetate 10:1 as the eluent). White solid (22.9 mg, 55% yield). m.p.: 160–162°C. ¹H NMR (400 MHz, CDCl₃, TMS) δ 8.94 (s, 1H), 7.65 (d, *J* = 7.2 Hz, 1H), 7.56–7.47 (m, 6H), 7.41–7.37 (m, 2H), 7.32–7.22 (m, 3H), 7.17–7.11 (m, 3H), 6.93 (d, *J* = 8.8 Hz, 2H), 5.04 (s, 1H), 3.88 (dt, *J* = 10.4 Hz, *J* = 4.4 Hz, 1H), 3.35 (td, *J* = 11.2 Hz, *J* = 4.0 Hz, 1H), 3.13–2.96 (m, 2H), 2.28 (s, 3H). ¹³C{¹H} NMR (100 MHz, CDCl₃, TMS) δ 170.7, 147.3, 140.5, 137.2, 136.8, 134.5, 132.1, 130.1, 129.0, 128.8, 127.8, 127.6, 127.5, 127.1, 126.8, 126.77, 120.1, 115.8, 66.5, 45.9, 28.8, 20.4. IR ν 3303, 3022, 2920, 2850, 1913, 1671, 1499, 1149 cm⁻¹. HRMS (ESI) *m/z*: calcd for C₂₉H₂₇N₂O [M+H]⁺ 419.2118; found 419.2119.

***N*-([1,1'-biphenyl]-4-yl)-2-(*m*-tolyl)-1,2,3,4-tetrahydroisoquinoline-1-carboxamide (3ha)**

Purified by silica gel chromatography (petroleum ether/ethyl acetate 10:1 as the eluent). White solid (19.3 mg, 46% yield). m.p.: 137–139°C. ¹H NMR (400 MHz, CDCl₃, TMS) δ 8.88 (s, 1H), 7.66–7.63 (m, 1H), 7.58–7.49 (m, 6H), 7.42–7.37 (m, 2H), 7.33–7.15 (m, 5H), 6.84–6.76 (m, 3H), 5.09 (s, 1H), 3.92 (dt, *J* = 11.2 Hz, *J* = 4.4 Hz, 1H), 3.40 (td, *J* = 10.4 Hz, *J* = 4.0 Hz, 1H), 3.14–2.99 (m, 2H), 2.35 (s, 3H). ¹³C{¹H} NMR (100 MHz, CDCl₃, TMS) δ 170.6, 149.5, 140.5, 139.4, 137.3, 136.8, 134.6, 132.2, 129.4, 129.2, 128.8, 127.7, 127.66, 127.5, 127.1, 126.85, 126.8, 121.3, 120.1, 116.0, 112.4, 66.4, 45.4, 28.8, 21.9. IR ν 3326, 3031, 2917, 2827, 1671, 1487, 1113, 835 cm⁻¹. HRMS (ESI) *m/z*: calcd for C₂₉H₂₆N₂O_{Na} [M+Na]⁺ 441.1937; found 441.1935.

***N*-([1,1'-biphenyl]-4-yl)-6,7-dimethoxy-2-phenyl-1,2,3,4-tetrahydroisoquinoline-1-carboxamide (3ia)**

Purified by silica gel chromatography (petroleum ether/ethyl acetate 2:1 as the eluent). Yellow solid (24.1 mg, 52% yield). m.p.: 197–198°C. ¹H NMR (400 MHz, CDCl₃, TMS) δ 8.85 (s, 1H), 7.56–7.48 (m, 6H), 7.42–7.37 (m, 2H), 7.35–7.28 (m, 3H), 7.18 (s, 1H), 7.03 (d, *J* = 8.0 Hz, 1H), 6.95 (dd, *J*₁ = *J*₂ = 7.2 Hz, 1H), 6.65 (s, 1H), 5.01 (s, 1H), 3.93–3.86 (m, 7H), 3.44–3.37 (m, 1H), 3.07–2.90 (m, 2H). ¹³C{¹H} NMR (100 MHz, CDCl₃, TMS) δ 170.8, 149.5, 148.5, 147.8, 140.5, 137.3, 136.8, 129.6, 128.8, 127.6, 127.1, 126.8, 126.6, 123.8, 120.5, 120.2, 115.6, 111.8, 110.6, 65.9, 56.1, 56.0, 45.6, 28.2. IR ν 3263, 3021, 2911, 2828, 1657, 1217, 1114, 992 cm⁻¹. HRMS (ESI) *m/z*: calcd for C₃₀H₂₉N₂O₃[M+H]⁺ 465.2173; found 465.2172.

***N*-([1,1'-biphenyl]-4-yl)-1-phenylpiperidine-2-carboxamide (3ja)**

Purified by silica gel chromatography (petroleum ether/ethyl acetate 10:1 as the eluent). White solid (11.4 mg 32% yield). m.p.: 139–141°C. ¹H NMR (400 MHz, CDCl₃, TMS) δ 8.45 (s, 1H), 7.55–7.48 (m, 6H), 7.41 (dd, *J*₁ = *J*₂ = 7.6 Hz, 2H), 7.33–7.29 (m, 3H), 7.07 (d, *J* = 8.0 Hz, 2H), 6.94 (dd, *J*₁ = *J*₂ = 7.2 Hz, 1H), 4.19 (t, *J* = 5.2 Hz, 1H), 3.36–3.34 (m, 2H), 2.21–2.17 (m, 1H), 2.01–1.94 (m, 1H), 1.80–1.61 (m, 5H). ¹³C{¹H} NMR (100 MHz, CDCl₃, TMS) δ 171.3, 150.7, 140.6, 137.1, 137.0, 129.6, 128.8, 127.6, 127.1, 126.8, 121.2, 120.0, 117.8, 62.8, 49.5, 26.4, 24.0, 21.7. IR ν 3323, 3025, 1671, 1484, 1241, 830, 759, 695. HRMS (ESI) *m/z*: calcd for C₂₄H₂₅N₂O [M+H]⁺ 357.1961; found 357.1958.

[(1,1'-biphenyl)-4-yl]-1-phenylpyrrolidine-2-carboxamide (3ka)

Purified by silica gel chromatography (petroleum ether/ethyl acetate 10:1 as the eluent). White solid (13.3 mg, 39% yield). m.p.: 207–208°C. ¹H NMR (400 MHz, CDCl₃, TMS) δ 8.44 (s, 1H), 7.59–7.51 (m, 6H), 7.41 (dd, *J*₁ = *J*₂ = 7.6 Hz, 2H), 7.33–7.27 (m, 3H), 6.89–6.84 (m, 1H), 6.73 (d, *J* = 8.0 Hz, 2H), 4.12–4.08 (m, 1H), 3.79–3.75 (m, 1H), 3.31–3.24 (m, 1H), 2.42–2.28 (m, 2H), 2.10–1.99 (m, 2H). ¹³C{¹H} NMR (100 MHz, CDCl₃, TMS) δ 172.3, 147.6, 140.5, 137.4, 136.6, 129.5, 128.8, 127.6, 127.2, 126.9, 120.3, 118.9, 113.5, 65.4, 50.1, 31.6, 24.4. IR ν 3326, 2967, 2818, 1663, 1497, 1005, 755, 713. HRMS (ESI) *m/z*: calcd for C₂₃H₂₃N₂O [M+H]⁺ 343.1875; found 343.1803.

***N*-(4-methoxyphenyl)-2-phenyl-1,2,3,4-tetrahydroisoquinoline-1-carboxamide (3ab)**

Purified by silica gel chromatography (petroleum ether/ethyl acetate 10:1 as the eluent). White solid (30.7 mg, 86% yield). m.p.: 132-134°C. ¹H NMR (400 MHz, CDCl₃, TMS) δ 8.70 (s, 1H), 7.63 (d, *J* = 8.4 Hz, 1H), 7.38-7.29 (m, 4H), 7.28-7.21 (m, 2H), 7.16 (d, *J* = 6.8 Hz, 1H), 6.99 (d, *J* = 8.0 Hz, 2H), 6.93 (dd, *J*₁ = *J*₂ = 6.8 Hz, 1H), 6.81-6.76 (m, 2H), 5.06 (s, 1H), 3.94-3.89 (m, 1H), 3.74 (s, 3H), 3.37 (td, *J* = 10.8 Hz, *J* = 4.0 Hz, 1H), 3.14-2.97 (m, 2H). ¹³C{¹H} NMR (100 MHz, CDCl₃, TMS) δ 170.3, 156.5, 149.5, 134.6, 132.2, 130.6, 129.5, 129.1, 127.7, 127.6, 126.8, 121.6, 120.2, 115.1, 114.0, 66.3, 55.5, 45.3, 28.8. IR ν 3298, 3029, 2900, 2850, 1498, 888, 814 cm⁻¹. HRMS (ESI) *m/z*: calcd for C₂₃H₂₃N₂O₂[M+H]⁺ 359.1754; found 359.1753.

***N*-(4-bromophenyl)-2-phenyl-1,2,3,4-tetrahydroisoquinoline-1-carboxamide (3ac)**

Purified by silica gel chromatography (petroleum ether/ethyl acetate 10:1 as the eluent). White solid (22.7 mg, 56% yield). m.p.: 154-155°C. ¹H NMR (400 MHz, CDCl₃, TMS) δ 8.83 (s, 1H), 7.61 (d, *J* = 8.8 Hz, 1H), 7.36-7.22 (m, 8H), 7.17 (d, *J* = 6.8 Hz, 1H), 7.00-6.92 (m, 3H), 5.06 (s, 1H), 3.91 (dt, *J* = 11.2 Hz, *J* = 4.4 Hz, 1H), 3.38 (td, *J* = 10.8 Hz, *J* = 4.0 Hz, 1H), 3.12-2.97 (m, 2H). ¹³C{¹H} NMR (100 MHz, CDCl₃, TMS) δ 170.7, 149.3, 136.5, 134.5, 131.9, 131.8, 129.6, 129.1, 127.81, 127.8, 126.9, 121.4, 120.5, 117.0, 115.3, 66.3, 45.4, 28.7. IR ν 3298, 3028, 2915, 2228, 1597, 1320, 992, 690 cm⁻¹. HRMS (ESI) *m/z*: calcd for C₂₂H₂₀N₂OBr [M+H]⁺ 407.0754; found 407.0752.

***N*-(4-iodophenyl)-2-phenyl-1,2,3,4-tetrahydroisoquinoline-1-carboxamide (3ad)**

Purified by silica gel chromatography (petroleum ether/ethyl acetate 10:1 as the eluent). White solid (19.0 mg, 42% yield). m.p.: 122-124°C. ¹H NMR (400 MHz, CDCl₃, TMS) δ 8.80 (s, 1H), 7.63-7.59 (m, 1H), 7.57-7.53 (m, 2H), 7.35-7.22 (m, 6H), 7.18-7.15 (m, 1H), 7.00-6.92 (m, 3H), 5.06 (s, 1H), 3.90 (dt, *J* = 11.2 Hz, *J* = 4.8 Hz, 1H), 3.42-3.35 (m, 1H), 3.11-2.97 (m, 2H). ¹³C{¹H} NMR (100 MHz, CDCl₃, TMS) δ 170.6, 149.3, 137.8, 137.2, 134.5, 131.8, 129.6, 129.1, 127.8, 127.77, 126.9, 121.7, 120.6, 115.4, 87.6, 66.4, 45.4, 28.7. IR ν 3323, 3027, 2919, 2242, 2242, 1597, 1178, 818 cm⁻¹. HRMS (ESI) *m/z*: calcd for C₂₂H₂₀N₂OI [M+H]⁺ 455.0615; found 455.0614.

***N*-(4-cyanophenyl)-2-phenyl-1,2,3,4-tetrahydroisoquinoline-1-carboxamide (3ae)**

Purified by silica gel chromatography (petroleum ether/ethyl acetate 10:1 as the eluent). White solid (18.1 mg, 51% yield). m.p.: 74-76°C. ¹H NMR (400 MHz, CDCl₃, TMS) δ 9.05 (s, 1H), 7.62-7.58 (m, 3H), 7.55-7.51 (m, 2H), 7.36-7.30 (m, 2H), 7.28-7.24 (m, 2H), 7.19-7.16 (m, 1H), 7.02-6.94 (m, 3H), 5.09 (s, 1H), 3.91 (dt, *J* = 11.2 Hz, *J* = 4.8 Hz, 1H), 3.43-3.36 (m, 1H), 3.11-2.98 (m, 2H). ¹³C{¹H} NMR (100 MHz, CDCl₃, TMS) δ 171.2, 149.2, 141.4, 134.5, 133.2, 131.4, 129.7, 129.1, 129.0, 128.0, 127.9, 126.9, 120.9, 119.7, 118.8, 115.6, 107.3, 66.4, 45.6, 28.7. IR ν 3323, 3030, 2915, 2224, 1921, 1672, 1402, 933 cm⁻¹. HRMS (ESI) *m/z*: calcd for C₂₃H₂₀N₃O [M+H]⁺ 354.1601; found 354.1602.

***N*-(3-cyanophenyl)-2-phenyl-1,2,3,4-tetrahydroisoquinoline-1-carboxamide (3af)**

Purified by silica gel chromatography (petroleum ether/ethyl acetate 10:1 as the eluent). White solid (15.5 mg, 43% yield). m.p.: 138-140°C. ¹H NMR (400 MHz, CDCl₃, TMS) δ 8.97 (s, 1H), 7.88-7.87 (m, 1H), 7.67-7.60 (m, 2H), 7.37-7.31 (m, 4H), 7.30-7.23 (m, 2H), 7.19-7.16 (m, 1H), 7.02-6.94 (m, 3H), 5.09 (s, 1H), 3.92 (dt, *J* = 11.2 Hz, *J* = 4.4 Hz, 1H), 3.42-3.35 (m, 1H), 3.13-2.99 (m, 2H). ¹³C{¹H} NMR (100 MHz, CDCl₃, TMS) δ 171.2, 149.3, 138.3, 134.5, 131.5, 129.8, 129.7, 129.0, 127.94, 127.9, 127.8, 126.9, 123.9, 123.0, 120.8, 118.3, 115.5, 113.0, 66.3, 45.6, 28.7. IR ν 3298, 3043, 2899, 2251, 2227, 1499, 1036, 888 cm⁻¹. HRMS (ESI) *m/z*: calcd for C₂₃H₂₀N₃O [M+H]⁺ 354.1601; found 354.1599.

***N*-(4-nitrophenyl)-2-phenyl-1,2,3,4-tetrahydroisoquinoline-1-carboxamide (3ag)**

Purified by silica gel chromatography (petroleum ether/ethyl acetate 5:1 as the eluent). Yellow oil (20.8 mg, 56% yield). ¹H NMR (400 MHz, CDCl₃, TMS) δ 9.19 (s, 1H), 8.13 (d, *J* = 9.2 Hz, 2H), 7.67-7.60 (m, 3H), 7.34-7.25 (m, 5H), 7.18 (d, *J* = 6.8 Hz, 1H), 7.02-6.95 (m, 3H), 5.11 (s, 1H), 3.96-3.89 (m, 1H), 3.43-3.38 (m, 1H), 3.11-3.01 (m, 2H). ¹³C{¹H} NMR (100 MHz, CDCl₃, TMS) δ 171.3, 149.2, 143.7, 143.2, 134.5, 131.3, 129.7, 129.0, 128.04, 128.0, 127.0, 121.0, 119.3, 115.7, 66.4, 45.7, 28.6.

***N*-([1,1'-biphenyl]-2-yl)-2-phenyl-1,2,3,4-tetrahydroisoquinoline-1-carboxamide (3ah)**

Purified by silica gel chromatography (petroleum ether/ethyl acetate 10:1 as the eluent). White solid (31.1 mg, 77% yield). m.p.: 53-54°C. ¹H NMR (400 MHz, CDCl₃, TMS) δ 9.18 (s, 1H), 8.50 (d, *J* = 8.4 Hz, 1H), 7.58 (d, *J* = 7.2 Hz, 1H), 7.34-7.24 (m, 4H), 7.23-7.13 (m, 5H), 7.09 (d, *J* = 7.2 Hz, 1H), 7.05-7.02 (m,

3H), 6.91 (dd, $J_1 = J_2 = 7.2$ Hz, 1H), 6.77 (d, $J = 8.0$ Hz, 2H), 4.91 (s, 1H), 3.28 (dt, $J = 10.8$ Hz, $J = 3.6$ Hz, 1H), 2.98 (td, $J = 10.8$ Hz, $J = 3.2$ Hz, 1H), 2.67 (dt, $J = 10.2$ Hz, $J = 3.2$ Hz, 1H), 2.46-2.38 (m, 1H). $^{13}\text{C}\{^1\text{H}\}$ NMR (100 MHz, CDCl_3 , TMS) δ 170.5, 148.9, 137.8, 135.0, 134.4, 132.1, 131.7, 129.6, 129.3, 129.2, 129.1, 128.9, 128.8, 128.5, 127.7, 127.6, 127.5, 126.9, 123.8, 119.7, 119.3, 114.4, 66.6, 44.3, 28.6. IR ν 3323, 3028, 2916, 2242, 1672, 1489, 1295, 1037 cm^{-1} . HRMS (ESI) m/z : calcd for $\text{C}_{28}\text{H}_{25}\text{N}_2\text{O}$ $[\text{M}+\text{H}]^+$ 405.1961; found 405.1960.

N-(4'-methoxy-[1,1'-biphenyl]-2-yl)-2-phenyl-1,2,3,4-tetrahydroisoquinoline-1-carboxamide (3ai)

Purified by silica gel chromatography (petroleum ether/ethyl acetate 10:1 as the eluent). White solid (36.4 mg, 84% yield). m.p.: 128-130°C. ^1H NMR (400 MHz, CDCl_3 , TMS) δ 9.17 (s, 1H), 8.46 (dd, $J_1 = 8.0$ Hz, $J_2 = 0.8$ Hz, 1H), 7.58 (d, $J = 7.2$ Hz, 1H), 7.32-7.26 (m, 3H), 7.25-7.17 (m, 2H), 7.15-7.12 (m, 1H), 7.10-7.05 (m, 2H), 6.98-6.89 (m, 3H), 6.77 (d, $J = 8.0$ Hz, 2H), 6.71-6.67 (m, 2H), 3.82 (s, 3H), 3.34 (dt, $J = 10.8$ Hz, $J = 4.0$ Hz, 1H), 3.03 (td, $J = 11.2$ Hz, $J = 3.6$ Hz, 1H), 2.73 (dt, $J = 16.0$ Hz, $J = 3.2$ Hz, 1H), 2.58-2.50 (m, 1H). $^{13}\text{C}\{^1\text{H}\}$ NMR (100 MHz, CDCl_3 , TMS) δ 170.4, 159.0, 148.9, 135.1, 134.5, 132.2, 131.4, 130.3, 129.8, 129.7, 129.3, 128.8, 128.2, 127.6, 127.4, 126.9, 123.7, 119.6, 119.3, 114.3, 114.1, 66.6, 55.3, 44.3, 28.6. IR ν 3316, 3061, 2914, 2846, 2247, 1598, 1035, 834 cm^{-1} . HRMS (ESI) m/z : calcd for $\text{C}_{29}\text{H}_{27}\text{N}_2\text{O}_2$ $[\text{M}+\text{H}]^+$ 435.2067; found 435.2068.

N-(4'-methyl-[1,1'-biphenyl]-2-yl)-2-phenyl-1,2,3,4-tetrahydroisoquinoline-1-carboxamide (3aj)

Purified by silica gel chromatography (petroleum ether/ethyl acetate 10:1 as the eluent). White solid (30.5 mg, 73% yield). m.p.: 136-138°C. ^1H NMR (400 MHz, CDCl_3 , TMS) δ 9.17 (s, 1H), 8.46 (d, $J = 9.6$ Hz, 1H), 7.56 (d, $J = 7.2$ Hz, 1H), 7.32-7.12 (m, 6H), 7.10-7.04 (m, 2H), 6.98 (d, $J = 8.0$ Hz, 2H), 6.94-6.88 (m, 3H), 6.73 (d, $J = 8.0$ Hz, 2H), 4.90 (s, 1H), 3.29 (dt, $J = 10.4$ Hz, $J = 4.4$ Hz, 1H), 3.02 (td, $J = 11.2$ Hz, $J = 3.2$ Hz, 1H), 2.70 (dt, $J = 15.6$ Hz, $J = 3.6$ Hz, 1H), 2.54-2.45 (m, 1H), 2.37 (s, 3H). $^{13}\text{C}\{^1\text{H}\}$ NMR (100 MHz, CDCl_3 , TMS) δ 170.3, 148.9, 137.4, 135.1, 134.7, 134.5, 132.2, 131.8, 129.6, 129.5, 129.2, 129.0, 128.9, 128.3, 127.6, 127.5, 126.9, 123.7, 119.7, 119.3, 114.3, 66.5, 44.3, 28.5, 21.3. IR ν 3327, 3057, 2950, 2917, 1683, 1493, 1271, 930 cm^{-1} . HRMS (ESI) m/z : calcd for $\text{C}_{29}\text{H}_{27}\text{N}_2\text{O}$ $[\text{M}+\text{H}]^+$ 419.2118; found 419.2116.

N-([1,1':4',1''-terphenyl]-2-yl)-2-phenyl-1,2,3,4-tetrahydroisoquinoline-1-carboxamide (3ak)

Purified by silica gel chromatography (petroleum ether/ethyl acetate 10:1 as the eluent). White solid (38.4 mg, 80% yield). m.p.: 119-121°C. ^1H NMR (400 MHz, CDCl_3 , TMS) δ 9.23 (s, 1H), 8.50 (dd, $J_1 = 8.8$ Hz, $J_2 = 1.2$ Hz, 1H), 7.65-7.61 (m, 2H), 7.58 (d, $J = 7.2$ Hz, 1H), 7.54-7.49 (m, 2H), 7.44-7.39 (m, 3H), 7.36-7.31 (m, 1H), 7.28-7.16 (m, 5H), 7.13-7.08 (m, 3H), 7.04 (d, $J = 7.2$ Hz, 1H), 6.90 (dd, $J_1 = J_2 = 7.2$ Hz, 1H), 6.75 (d, $J = 8.0$ Hz, 2H), 4.92 (s, 1H), 3.28 (dt, $J = 10.4$ Hz, $J = 4.4$ Hz, 1H), 2.98 (td, $J = 11.2$ Hz, $J = 3.2$ Hz, 1H), 2.68 (dt, $J = 15.6$ Hz, $J = 3.6$ Hz, 1H), 2.55-2.46 (m, 1H). $^{13}\text{C}\{^1\text{H}\}$ NMR (100 MHz, CDCl_3 , TMS) δ 170.4, 148.9, 140.4, 140.3, 136.7, 135.0, 134.4, 132.2, 131.4, 129.6, 129.54, 129.5, 129.3, 129.0, 128.9, 128.6, 127.7, 127.6, 127.53, 127.5, 127.4, 127.1, 127.0, 126.9, 123.8, 119.8, 119.4, 114.4, 66.6, 44.4, 28.5. IR ν 3300, 3025, 2849, 2247, 1685, 1111, 906, 841 cm^{-1} . HRMS (ESI) m/z : calcd for $\text{C}_{34}\text{H}_{29}\text{N}_2\text{O}$ $[\text{M}+\text{H}]^+$ 481.2274; found 481.2273.

N-benzyl-2-phenyl-1,2,3,4-tetrahydroisoquinoline-1-carboxamide (3al)

Purified by silica gel chromatography (petroleum ether/ethyl acetate 10:1 as the eluent). White solid (29.3 mg, 86% yield). m.p.: 154-156°C. ^1H NMR (400 MHz, CDCl_3 , TMS) δ 7.64-7.61 (m, 1H), 7.32-7.14 (m, 9H), 7.04-7.00 (m, 2H), 6.93-6.88 (m, 3H), 5.06 (s, 1H), 4.43-4.32 (m, 2H), 3.82 (dt, $J = 10.8$ Hz, $J = 4.4$ Hz, 1H), 3.28 (td, $J = 10.4$ Hz, $J = 3.6$ Hz, 1H), 3.07-2.91 (m, 2H). $^{13}\text{C}\{^1\text{H}\}$ NMR (100 MHz, CDCl_3 , TMS) δ 172.4, 149.4, 138.1, 134.5, 132.6, 129.4, 128.9, 128.6, 127.7, 127.5, 127.4, 127.3, 126.8, 119.7, 114.9, 65.6, 45.2, 43.4, 29.0. IR ν 3319, 3025, 2831, 2247, 1489, 1055, 903, 756 cm^{-1} . HRMS (ESI) m/z : calcd for $\text{C}_{23}\text{H}_{23}\text{N}_2\text{O}$ $[\text{M}+\text{H}]^+$ 343.1805; found 343.1803.

N-phenethyl-2-phenyl-1,2,3,4-tetrahydroisoquinoline-1-carboxamide (3am)

Purified by silica gel chromatography (petroleum ether/ethyl acetate 5:1 as the eluent). White solid (19.9 mg, 56% yield). m.p.: 123-125°C. ^1H NMR (400 MHz, CDCl_3 , TMS) δ 7.60-7.57 (m, 1H), 7.32-7.23 (m, 4H), 7.19-7.11 (m, 4H), 6.93-6.84 (m, 6H), 4.94 (s, 1H), 3.71 (dt, $J = 11.2$ Hz, $J = 4.0$ Hz, 1H), 3.52-3.36 (m, 2H), 3.19 (td, $J = 11.2$ Hz, $J = 3.6$ Hz, 1H), 2.89-2.60 (m, 4H). $^{13}\text{C}\{^1\text{H}\}$ NMR (100 MHz, CDCl_3 , TMS) δ 172.3, 149.2, 138.7, 134.6, 132.6, 129.4, 128.8, 128.7, 128.5, 127.5, 127.46, 126.8, 126.4, 119.4, 114.3, 65.6, 44.6, 40.6, 35.4, 28.8. IR ν 3298, 3028, 2899, 2228, 1663, 1516, 943, 791 cm^{-1} . HRMS (ESI) m/z : calcd for $\text{C}_{24}\text{H}_{25}\text{N}_2\text{O}$ $[\text{M}+\text{H}]^+$ 357.1961; found 357.1960.

***N*-(4-methylphenethyl)-2-phenyl-1,2,3,4-tetrahydroisoquinoline-1-carboxamide (3an)**

Purified by silica gel chromatography (petroleum ether/ethyl acetate 5:1 as the eluent). White solid (28.5 mg, 77% yield). m.p.: 97–99°C. ¹H NMR (400 MHz, CDCl₃, TMS) δ 7.59–7.56 (m, 1H), 7.31–7.21 (m, 4H), 7.14–7.11 (m, 1H), 6.97 (d, *J* = 7.6 Hz, 2H), 6.90–6.79 (m, 6H), 4.93 (s, 1H), 3.71 (dt, *J* = 11.2 Hz, *J* = 4.8 Hz, 1H), 3.49–3.34 (m, 2H), 3.20 (td, *J* = 10.4 Hz, *J* = 4.4 Hz, 1H), 2.90–2.75 (m, 2H), 2.71–2.55 (m, 2H), 2.29 (s, 3H). ¹³C{¹H} NMR (100 MHz, CDCl₃, TMS) δ 172.3, 149.3, 135.8, 135.6, 134.6, 132.7, 129.4, 129.2, 128.9, 128.7, 128.6, 127.5, 127.4, 126.7, 119.4, 114.3, 65.6, 44.7, 40.7, 35.0, 28.8, 21.0. IR ν 3262, 3063, 2831, 2241, 1598, 1442, 1426, 987 cm⁻¹. HRMS (ESI) *m/z*: calcd for C₂₅H₂₇N₂O [M+H]⁺ 371.2118; found 371.2120.

***N*-(3,4-dimethoxyphenethyl)-2-phenyl-1,2,3,4-tetrahydroisoquinoline-1-carboxamide (3ao)**

Purified by silica gel chromatography (petroleum ether/ethyl acetate 2:1 as the eluent). White solid (23.3 mg, 56% yield). m.p.: 105–106°C. ¹H NMR (400 MHz, CDCl₃, TMS) δ 7.58–7.55 (m, 1H), 7.31–7.20 (m, 4H), 7.13–7.10 (m, 1H), 6.93–6.82 (m, 4H), 6.66 (d, *J* = 8.4 Hz, 1H), 6.54 (d, *J* = 2.0 Hz, 1H), 6.46 (dd, *J* = 8.0 Hz, *J* = 1.6 Hz, 1H), 4.93 (s, 1H), 3.84 (s, 3H), 3.72–3.65 (m, 4H), 3.48–3.41 (m, 2H), 3.20 (td, *J* = 11.2 Hz, *J* = 3.6 Hz, 1H), 2.89–2.57 (m, 4H). ¹³C{¹H} NMR (100 MHz, CDCl₃, TMS) δ 172.3, 149.3, 148.9, 147.5, 134.5, 132.7, 131.1, 129.4, 128.9, 127.5, 127.4, 126.7, 120.6, 119.4, 114.2, 111.6, 111.2, 65.7, 55.9, 55.7, 44.6, 40.5, 35.0, 28.8. IR ν 3028, 2915, 2850, 2251, 1662, 1061, 889, 752 cm⁻¹. HRMS (ESI) *m/z*: calcd for C₂₆H₂₉N₂O₃[M+H]⁺ 417.2173; found 417.2171.

2-phenyl-*N*-(4-phenylbutyl)-1,2,3,4-tetrahydroisoquinoline-1-carboxamide (3ap)

Purified by silica gel chromatography (petroleum ether/ethyl acetate 5:1 as the eluent). White solid (23.8 mg, 62% yield). m.p.: 146–148°C. ¹H NMR (400 MHz, CDCl₃, TMS) δ 7.60–7.57 (m, 1H), 7.31–7.19 (m, 6H), 7.17–7.12 (m, 2H), 7.05–7.02 (m, 2H), 6.91–6.84 (m, 4H), 4.96 (s, 1H), 3.83 (dt, *J* = 11.2 Hz, *J* = 4.4 Hz, 1H), 3.31–3.11 (m, 3H), 3.06–2.91 (m, 2H), 2.50 (t, *J* = 6.8 Hz, 2H), 1.51–1.36 (m, 4H). ¹³C{¹H} NMR (100 MHz, CDCl₃, TMS) δ 172.2, 149.4, 142.1, 134.4, 132.8, 129.4, 128.9, 128.3, 127.5, 127.4, 126.8, 125.7, 119.6, 114.5, 65.6, 45.0, 39.2, 35.4, 29.1, 29.0, 28.5. IR ν 3254, 3061, 2941, 2828, 1676, 1559, 1217, 827 cm⁻¹. HRMS (ESI) *m/z*: calcd for C₂₆H₂₉N₂O [M+H]⁺ 385.2274; found 385.2272.

***N*-octyl-2-phenyl-1,2,3,4-tetrahydroisoquinoline-1-carboxamide (3aq)**

Purified by silica gel chromatography (petroleum ether/ethyl acetate 5:1 as the eluent). White solid (32.8 mg, 90% yield). m.p.: 129–130°C. ¹H NMR (400 MHz, CDCl₃, TMS) δ 7.60–7.57 (m, 1H), 7.32–7.27 (m, 2H), 7.25–7.19 (m, 2H), 7.15–7.12 (m, 1H), 6.92–6.87 (m, 4H), 4.97 (s, 1H), 3.85 (dt, *J* = 10.8 Hz, *J* = 4.0 Hz, 1H), 3.28 (td, *J* = 10.8 Hz, *J* = 4.0 Hz, 1H), 3.23–3.11 (m, 2H), 3.10–2.94 (m, 2H), 1.41–1.32 (m, 2H), 1.26–1.10 (m, 11H), 0.86 (t, *J* = 7.2 Hz, 3H). ¹³C{¹H} NMR (100 MHz, CDCl₃, TMS) δ 172.1, 149.4, 134.4, 132.8, 129.4, 128.9, 127.5, 127.4, 126.7, 119.5, 114.5, 65.6, 45.0, 39.5, 31.7, 29.5, 29.2, 29.1, 29.0, 26.8, 22.6, 14.1. IR ν 3264, 3060, 2950, 2847, 1673, 1425, 1220, 1053 cm⁻¹. HRMS (ESI) *m/z*: calcd for C₂₄H₃₃N₂O [M+H]⁺ 365.2587; found 365.2585.

***N*-dodecyl-2-phenyl-1,2,3,4-tetrahydroisoquinoline-1-carboxamide (3ar)**

Purified by silica gel chromatography (petroleum ether/ethyl acetate 5:1 as the eluent). White solid (32.3 mg, 77% yield). m.p.: 101–103°C. ¹H NMR (400 MHz, CDCl₃, TMS) δ 7.61–7.57 (m, 1H), 7.33–7.20 (m, 4H), 7.16–7.13 (m, 1H), 6.92–6.87 (m, 4H), 4.97 (s, 1H), 3.86 (dt, *J* = 10.8 Hz, *J* = 4.4 Hz, 1H), 3.30 (td, *J* = 10.8 Hz, *J* = 4.0 Hz, 1H), 3.25–3.11 (m, 2H), 3.10–2.94 (m, 2H), 1.43–1.12 (m, 20H), 0.88 (t, *J* = 7.2 Hz, 3H). ¹³C{¹H} NMR (100 MHz, CDCl₃, TMS) δ 172.1, 149.4, 134.4, 132.8, 129.4, 128.9, 127.5, 127.4, 126.7, 119.5, 114.5, 65.6, 44.9, 39.5, 31.9, 29.65, 29.64, 29.54, 29.51, 29.49, 29.4, 29.2, 29.0, 26.8, 22.7, 14.2. IR ν 3317, 3027, 2918, 2246, 1663, 1488, 904, 723 cm⁻¹. HRMS (ESI) *m/z*: calcd for C₂₈H₄₁N₂O [M+H]⁺ 421.3213; found 421.3212.

***Ethyl* (2-phenyl-1,2,3,4-tetrahydroisoquinoline-1-carbonyl)glycinate (3as)**

Purified by silica gel chromatography (petroleum ether/ethyl acetate 5:1 as the eluent). Colorless oil (31.1 mg, 92% yield). ¹H NMR (400 MHz, CDCl₃, TMS) δ 7.55–7.52 (m, 1H), 7.45–7.42 (m, 1H), 7.33–7.22 (m, 4H), 7.17–7.13 (m, 1H), 6.96–6.87 (m, 3H), 5.03 (s, 1H), 4.16–4.06 (m, 3H), 3.91–3.83 (m, 2H), 3.37–3.30 (m, 1H), 3.20–3.11 (m, 1H), 3.02–2.95 (m, 1H), 1.20 (t, *J* = 7.2 Hz, 3H). ¹³C{¹H} NMR (100 MHz, CDCl₃, TMS) δ 172.6, 169.6, 149.3, 135.0, 132.5, 129.4, 129.1, 127.6, 127.56, 126.7, 119.5, 114.4, 65.4, 61.5, 44.8, 41.3, 28.6, 14.1. IR ν 3298, 2918, 2250, 1598, 1318, 1036, 791, 692 cm⁻¹. HRMS (ESI) *m/z*: calcd for C₂₀H₂₃N₂O₃[M+H]⁺ 339.1703; found 339.1701.